FINAL REPORT
GRANGER ASSOCIATES
POINT-TO-POINT
LOG PERIODIC ANTENNA SYSTEM

This report has been approved for general distribution.

Prepared for
The Federal Aviation Agency
Research and Development Service

Contract ARDS-583
Serial No. RD-602-180-62
(FAA Project No. 113-23-1D)

FINAL REPORT

GRANGER ASSOCIATES

POINT-TO-POINT

LOG PERIODIC ANTENNA SYSTEM

Prepared for
The Federal Aviation Agency
Research and Development Service

Contract ARDS-583
Serial No. RD-602-180-62
(FAA Project No. 113-23-1D)

(Granger publ. no. 0066-1)

GRANGER ASSOCIATES
Palo Alto, California
January 1963

TABLE OF CONTENTS

ABSTRACT

The electrical characteristics of log periodic high frequency antennas installed for the Federal Aviation Agency Research and Development Service at Barnegat, New Jersey, and San Juan, Puerto Rico, sites are described. The antenna at Barnegat is a horizontally polarized Granger Associates Model 748 receiving antenna modified to meet special requirements of the FAA. The antenna at San Juan is a standard Granger Associates vertically polarized Model 726-2.5/30-T transmitting antenna.

The results of model radiation pattern measurements, impedance measurements, ground reflection calculations, and cable attenuation calculations are given for the Barnegat antenna. The general radiation pattern, results of impedance measurements, and cable attenuation calculations are given for the San Juan antenna. Calculated values of installed gain are derived for each antenna.

1. PURPOSE

Two antennas were supplied under this contract to permit evaluation of the effectiveness of high-frequency logarithmically periodic antennas for use by the Federal Aviation Agency Research and Development Service. The two antennas form a research link with transmission from San Juan, Puerto Rico, to Barnegat, New Jersey.

2. GENERAL FACTUAL DATA

a. General Description, Barnegat Receiving Antenna.

(1) The antenna installed at the Barnegat, New Jersey receiving site is a modified Granger Associates Model 748 Antenna designated as Model 748-3/30-15N. This antenna is a horizontally polarized two-curtain transposed dipole logarithmic periodic array, illustrated by figure 1. It was designed especially to meet the requirements of Federal Aviation Agency, Research and Development Service Specification "Modernization of HF Point-to-Point Antenna System" for use in Project 113-23-1D. Characteristics of the antenna are given in figure 2. A photograph of the antenna is shown in figure 3.

(2) The 748-3/30-15N antenna is installed with the main lobe of its radiation pattern oriented South 20.43° East to receive signals from the San Juan, Puerto Rico transmitting system. It is connected to the receiver through approximately 1400 feet of 7/8 inch Heliax (Andrew Corp.) 50 ohm coaxial cable.

b. General Description, San Juan Transmitting Antenna.

(1) The antenna installed at the San Juan (Cibuco), Puerto Rico transmitting site is a standard Granger Associates Model 726-2.5/30-T antenna. This is a vertically polarized monopole logarithmic periodic array, illustrated by figure 4. Characteristics of this antenna are given in figure 5.

(2) This antenna is installed with the main lobe of its radiation pattern oriented North 8.93° West. The antenna thus is directed about 11° east of the great circle path to the Barnegat receiving site. This deviation was made so that the antenna

could, if desired, be used in communication links with Miami, Florida and London, England. In this orientation the signal directed at Barnegat is negligibly different from that at the beam maximum.

(3) The antenna is connected to the transmitter through approximately 1900 feet of 1-5/8 inch Heliax (Andrew Corp.) 50 ohm coaxial cable.

c. Tests on the Barnegat Receiving Antenna.

(1) The 748-3/30-15N antenna represented a modification to a standard design. For this reason laboratory tests, in addition to the usual field check tests, were performed to verify the correctness of the antenna design.

(2) Scale model radiation pattern measurements using imaging techniques were conducted to obtain data on the directivity, beam maximum elevation angles, and beamwidth of the antenna. Free-space model radiation patterns were also measured at selected frequencies and used to compute the effect of imperfect earth on the performance of the antenna as installed at the Barnegat site.

(3) Field tests consisted of visual inspection of the antenna, impedance measurements at the antenna terminals and at the receiver end of the transmission line, and simple listening tests to verify the correctness of the installation.

(4) Measurement data were used to calculate the overall performance of the installed antenna as an aid to the FAA Research and Development Service evaluation program under Project 113-23-1D.

d. Tests on San Juan Transmitting Antenna.

(1) The Model 726-2.5/30-T antenna is of well established design. For this reason only field check-out tests were conducted. These tests consisted of visual inspection of the antenna, impedance measurements at the antenna terminals and at the transmitter end of the transmission line, and simple transmitter loading tests.

(2) The overall performance of the installed antenna was calculated as an aid to the Project 113-23-1D evaluation program.

3. DETAILED FACTUAL DATA

a. Radiation Patterns of Barnegat antenna.

(1) Two principal groups of radiation patterns were measured: imaging and free-space radiation.

(2) The primary group of patterns, figure 6, were measured using imaging techniques: a second antenna, properly phased with respect to the principal antenna was used to represent the effect of placing the antenna over a "perfect" earth. In the imaging process, the H-plane or vertical cut patterns show not only the patterns that actually would exist above ground but also a duplicate symmetrical pattern. The ground plane in the H-plane patterns is along the 0° - 180° axis on the paper.

(3) A word of explanation may be in order to assist in interpreting these radiation patterns. The H-plane patterns correspond to vertical plane cuts through the antenna fore and aft centerline and show the vertical plane variation of radiation, plotted on a voltage basis. The E-plane patterns are azimuth cuts and show azimuthal variation of radiation on a voltage basis. The radiation intensity of a horizontally polarized antenna in the plane of the ground is zero. For this reason the E-plane (azimuth) cuts were made at angles above the horizontal that closely approximated the angle of maximum radiation. The high frequency (13.1 to 30 Mc) E-plane patterns were cut at an angle of 15° above the horizon; the low frequency (3.0 to 7.61 Mc) E-plane patterns were cut at an angle of 25° above the horizon.

(4) Because of limitations imposed by the large size of the antenna, two sets of patterns were measured using the same groups of radiator elements. One set designated as 1/27.122 scale, describes the patterns that would be obtained

between full scale frequencies of 13.1 and 30 Mc. In this set the modeling of the antenna was complete; that is, radiator diameters and transmission line configuration were exactly scaled. The spacings between radiators, the radiator lengths, the spacings between bays, and the spacings between bays and ground exactly simulated those which are used at the front (high frequency) end of the full scale antenna.

(5) The second set of patterns, designated as 1/118.547 scale describes the patterns that would be obtained between full scale frequencies of 3.0 and 7.61 Mc. In this set the modeling was only partially complete. The spacings between radiators, radiator lengths, the spacings between bays and between bays and ground exactly simulated those which are used at the rear (low frequency) end of the full scale antenna. The transmission line wire size and conductor spacing, and radiator diameters were made to 1/27.122 scale and were thus not exactly modeled for this set of patterns. The departure from exact modeling of these details, however, is small enough that the patterns are entirely valid.

(6) The directive gain, elevation angle of maximum radiation, and side and back lobe levels of the antenna were derived from the foregoing radiation pattern data and are presented in figures 7, 8 and 9. The directive gain was calculated by an approximate integration process using the radiation patterns as basic data. All of these characteristics are those that would be obtained over a perfect earth.

(7) A secondary group of scale model patterns was measured for the 748-3/30-15N antenna and are shown in figure 10. These patterns represent the free-space radiation (radiation in the absence of earth) of the antenna. Modeling and procedures were the same as for the imaged patterns except that no image antenna was used. In the case of the H-plane vertical cut patterns, the measurements were made with the midline of the antenna bays (a line drawn half way between the bays) pointed at the 0° reference. In the actual installation of the antenna, the midline

makes an angle of 15.01° with the earth, hence the line of earth will be at the 15.01° point on these patterns.

(8) These free space vertical cut radiation patterns were used in computing the vertical plane patterns and the losses to be expected with the antenna operating over an imperfect, rather than a perfect earth.

b. Ground Reflection calculations for the Barnegat Receiving Antenna.

(1) To calculate the radiation patterns over imperfect earth, consider the geometry of figure 11.

(1)

Then

$$\left|E_{(\theta)}\right| = \left[A^2 + (Br)^2 - 2ABr\cos\left(\frac{4\pi h}{\lambda}\sin\theta - \rho\right)\right]^{1/2}$$

Where $\left|E_{(\theta)}\right|$ is the resultant relative field strength at an angle of elevation above earth.

A is the relative field strength of the free space vertical plane pattern at elevation angle θ .

B is the relative field strength of the free space vertical plane pattern at depression angle θ .

r is the magnitude of the earth reflection coefficient at elevation angle θ .

$\frac{h}{\lambda}$ is the height of the (free space) antenna phase center in wavelengths.

ρ is the angle by which the phase of the reflected wave leads the phase that it would have in the case of perfect earth.

(2) For the 748-3/30-15N antenna the phase center height is given approximately by the formula

$$\frac{h}{\lambda} \simeq \frac{20.7704}{\lambda} + .385429 \qquad (2)$$

(3) The reflection coefficient magnitude r and phase angle ρ are functions of the earth conductivity σ, dielectric constant ϵ, frequency and angle of incidence θ. For the Barnegat, New Jersey site values of σ = 4 millimhos/meter and ϵ = 10 are appropriate[1,2].

The values of the reflection coefficient $r\angle\rho$ may be calculated from the formula:[2]

$$r\angle\rho = \left[(\epsilon' - \cos^2\theta)^{1/2} - \sin\theta\right] \div \left[(\epsilon' - \cos^2\theta)^{1/2} + \sin\theta\right] \qquad (3)$$

where $\epsilon' = \epsilon - j\,0.06\,\sigma\lambda$

ϵ = dielectric constant with air as unity

σ = millimhos per meter conductivity

λ = wavelength

(4) Theoretical vertical plane radiation patterns were computed for frequencies of 3.0, 5.07, 14.77 and 29.5 Mc. Plots of these patterns are given in figure 12. These patterns may be compared with patterns measured by the image method which indicate the performance over a "perfect" earth. The principal effect of imperfect earth is to reduce the efficiency of the antenna. The efficiency due to imperfect earth is given approximately by the equation: $\eta_{\theta\,max} \simeq \left(\frac{A+Br}{A+B}\right)^2$

where θ max is the elevation angle of maximum radiation.

The efficiency η for the 748-3/30-15N antenna at the Barnegat site has been calculated and plotted in figure 13.

A secondary effect of imperfect earth is to reduce the elevation angle of maximum radiation. This results from the fact that ground currents penetrate the earth to an appreciable distance and as a consequence the effective height of the antenna is raised.

A third effect of imperfect earth is to narrow the beamwidth of the pattern in the vertical plane as a result of greater ground losses at higher angles of incidence.

c. Radiation Patterns of San Juan Antenna.

(1) The model 726-2.5/30-T antenna installed at San Juan, Puerto Rico is a standard Granger Associates antenna, hence radiation patterns were not measured especially for this program. The radiation patterns are, however, typically constant over the frequency range of 2.5 to 30 Mc. A typical set of radiation patterns, measured by model and imaging techniques to simulate performance over perfect earth, are given in figure 14.

(2) The efficiency of vertically polarized antennas over an imperfect earth depends greatly on the nature of the ground screen of the antenna. The effectiveness of the ground screen is difficult to measure to any great degree of accuracy. Calculations made for the 726-2.5/30-T antenna indicate an efficiency shown by figure 24 at an elevation angle of 8°. This elevation angle is assumed because it corresponds to that required for one-hop F layer propagation on the San Juan to Barnegat circuit.

d. Impedance measurements of the antennas.

Impedance measurements were conducted on both antennas. The test equipment used is shown in the block diagram of figure 15. Measurements were made at the input connector of the antenna and also at the transmitter or receiver end of the transmission line for each antenna. Results of the measurements are shown in tabular form in figures 16 and 17, and are shown graphically in figures 18 and 19. The voltage standing wave ratios are plotted in figure 20.

e. Transmission cable losses.

(1) The antennas are connected to their respective equipments through lengths of

coaxial transmission cable. The 748-3/30-15N antenna at Barnegat uses approximately 1400 feet of 7/8 inch diameter Andrew Corporation type H5-50 Heliax cable of 50 ohm characteristic impedance. The 726-2.5/30-T antenna at San Juan uses approximately 1900 feet of 1-5/8 inch diameter Andrew Corporation type H7-50 Heliax cable of 50 ohms characteristic impedance. Attenuation values for these cables are published. From these published values the attenuations for the particular length used are calculated and are shown in figure 21.

f. Calculated overall installed gain, Barnegat antenna.

(1) The overall gain of the barnegat antenna includes the factors of directive gain (directivity), imperfect ground losses, reflection losses due to mismatch, and cable attenuation losses. Expressed mathematically G_t = DLRA or in decibels

$G_{t_{db}} = D_{db} + L_{db} + R_{db} + A_{db}$ where G_t is the total gain

D is the directivity

L is the loss due to imperfect earth

R is the loss due to mismatch reflection

A is the loss due to cable attenuation

(2) The curve of directivity as a function of frequency is shown in figure 7. The curve of loss due to imperfect earth is shown in figure 13. The loss due to reflection is given by $R_{db} = 10 \log_{10} \frac{4\rho_t}{(\rho_t+1)^2}$ Where ρ is the voltage standing wave ratio at the antenna. The curve of ρ as a function of frequency is shown in figure 20. The cable attenuation is shown in figure 21. From these data the total installed gain $G_{t_{db}}$ has been calculated and is shown in figure 22.

(3) For the transmitting antenna at San Juan, the calculations are somewhat modified. Because practice is to match the transmitter to the input impedance of the transmission line reflection loss does not enter directly into the picture. In this case the overall gain is given by: $G_{t_{db}} = D_{db} + L_{db} + A'_{db}$

where A' is the increased attenuation losses caused by standing waves on the transmission line and is given by:

$$A'_{db} = -(\alpha l)_{db} + 10 \log_{10} \frac{4\rho_t}{(\rho+1)^2} - 10 \log_{10} \left\{ 1 - \left(\frac{\rho_t - 1}{\rho_t + 1}\right)^2 \exp\left[-(\alpha l)_{db}/2.17\right] \right\}$$

where: $(\alpha l)_{db}$ is the attenuation of the transmission line for a matched load

ρ_t is the voltage standing wave ratio at the antenna.

The directivity D_{db} for the 726-2.5/30-T antenna is assumed to be +9.87 db for an elevation angle of 8°. A plot of A'_{db} as a function of voltage standing wave ratio and line attenuation is shown in figure 23. The factor L_{db} is shown in figure 24.

(4) The total installed gain $G_{t_{db}}$ has been calculated for the 726-2.5/30-T antenna at San Juan, and is shown in figure 25.

4. CONCLUSIONS

a. Electrical measurements on the 748-3/30-15N and the 726-2.5/30-T antennas indicate that they satisfy the requirements of the governing Federal Aviation Agency Research and Development Service Specification[3] for use in Project 113-23-1D. Radiation pattern and directivity data for the 748-3/30-15N antenna at Barnegat compares closely with theoretical data, and shows a gratifying similarity to that predicted in the Granger Associates Proposal.[4]

b. The overall performance of the antennas has been calculated as an aid to the evaluation program to be conducted under project 113-23-1D.

5. ACKNOWLEDGEMENT

I would like to express my great appreciation to Mr. G. V. Rodgers, Mr. W. M. Smith, Mr. H. Charland, Mr. W. Thomas, Mr. T. Ducros and others of the Federal Aviation Agency for their encouragement and assistance in resolving questions associated with installation of these antennas.

W. E. Moore

6. REFERENCES

1. FCC Document 3.190, February 1954, figure R-3.
2. Terman, F. G.; "Radio Engineers Handbook", McGraw Hill, 1st Ed. 1943.
3. FAA Research and Development Service specification "Modernization of HF Point-to-Point Antenna System" for use in project 113-23-1D.
4. Granger Associates Technical Proposal 62.1695 for a 3-to-30 Mc Log-Periodic Antenna to the FAA in response to RFP No. DD-CB-060 Ser. RD-602-32-62.
5. Installation and Maintenance Manual Granger Associates Model 748-3/30-15N Log-Periodic Antenna, Publication No. 0025-1.

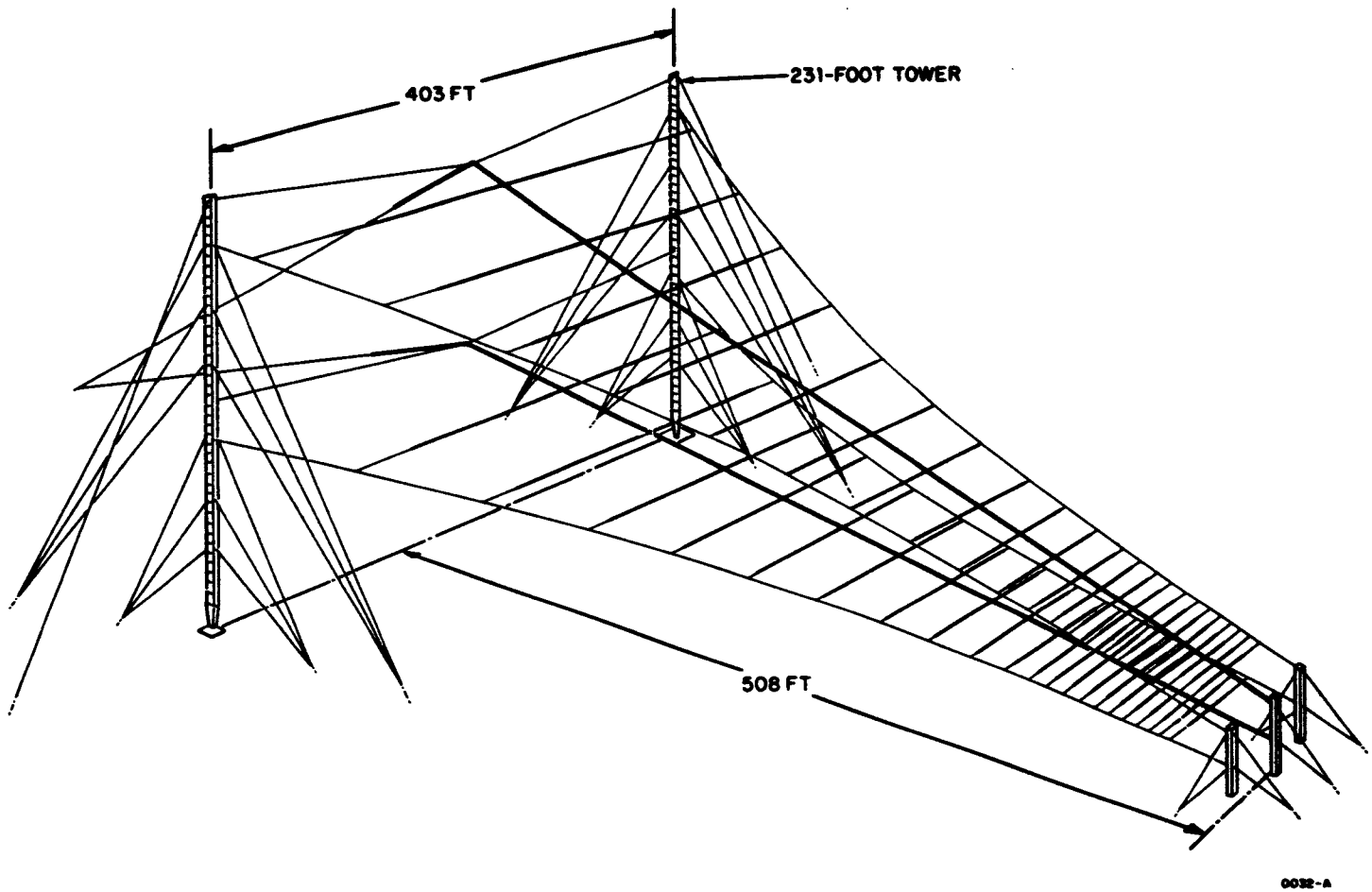

Figure 1. Isometric View of the 748-3/30-15N Antenna

Frequency Range	3-30 Mc
Polarization	Horizontal
VSWR	2:1 (Nominal)
Directive Gain (Over Isotropic Radiator)	3 to 5 Mc ≥13.5 db 5 to 15 Mc ≥14 db 15 to 30 Mc ≥15 db
Azimuth-Plane Beamwidth (Half-Power Points)	60 degrees nominal
Elevation-Plane Beamwidth (Half-Power Points)	3 Mc 32° 5 Mc 29° 15 Mc 20° 30 Mc 13°
Elevation Angle of Maximum Radiation	3 Mc 30° 5 Mc 27° 15 Mc 19° 30 Mc 12.5°
Back-to-Front Ratio and Sidelobe Level (excluding vertical bulge on main lobe)	Better than 15 db
Impedance	50 ohms through Model 538B-50/150 balun.
Transmission-Line Connector	Coaxial LC Type UG-352A/U (Model 538B-50/150 receiving Balun)
Power-Handling Capability	Receiving application.
Tower Height	230 feet
Site Area Requirement	725 x 735 feet (approx.)
Environment	100 mph wind with 1/2 inch radial ice.

Figure 2. Characteristics of the 748-3/30-15N Antenna

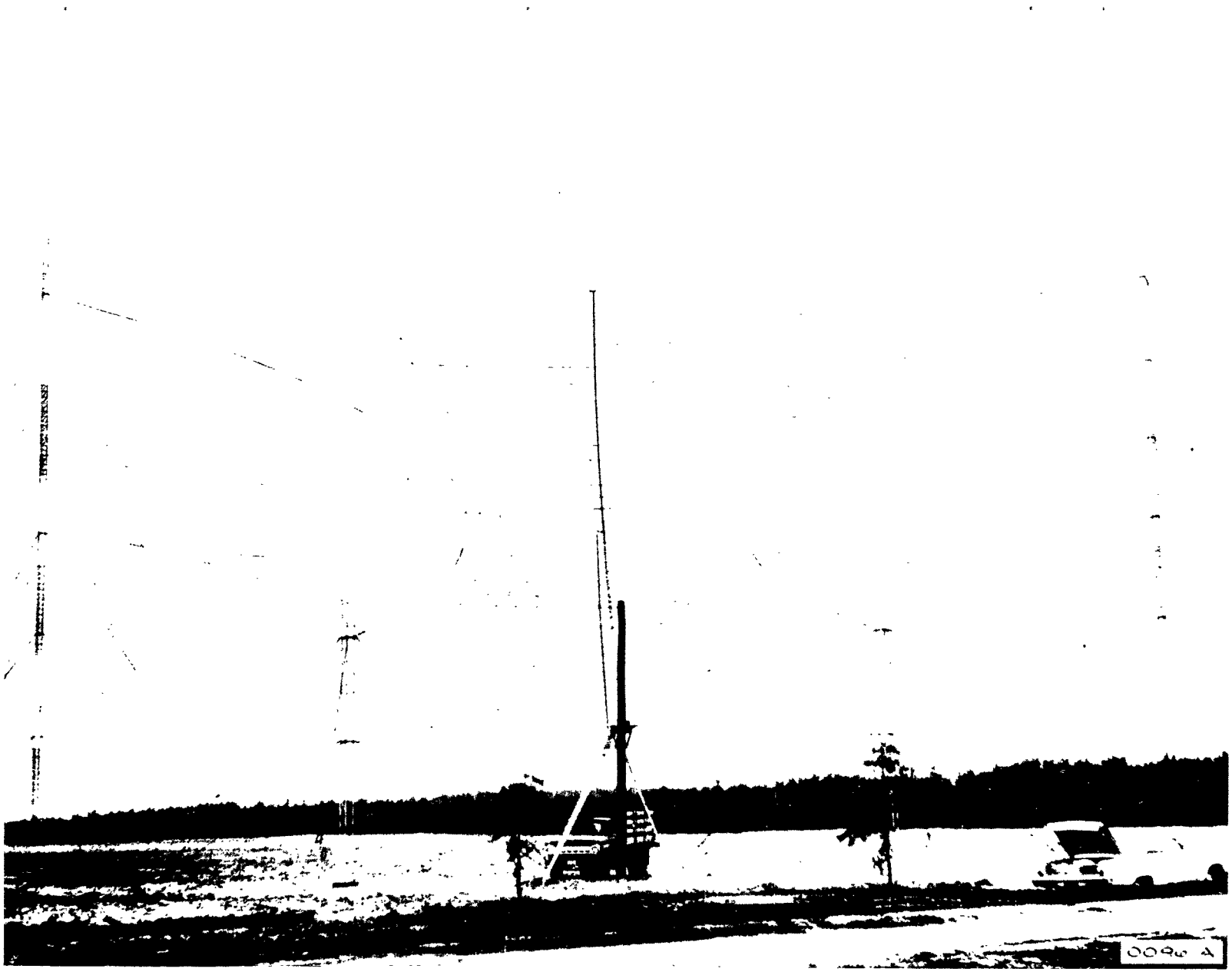

Figure 3. Photograph of the 748-3/30-15N Antenna.

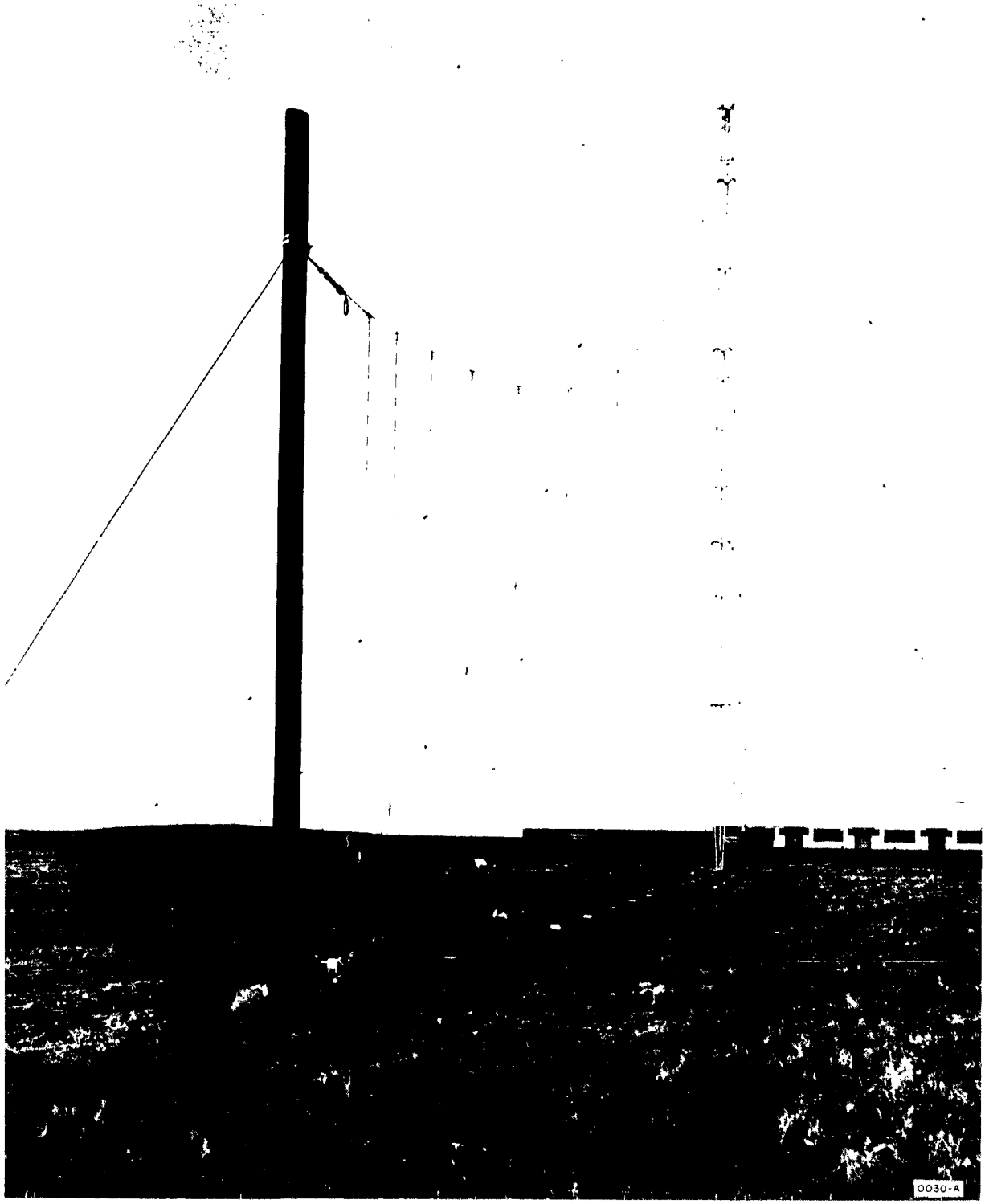

Figure 4. Photograph of the 726-2.5/30-T

Frequency Range:	2.5 - 30 Mc
Polarization:	Vertical
VSWR:	2:1 (Nominal)
Directive Gain (over isotropic radiator):	10 db
Azimuth-Plane Beamwidth: (Half-Power Points)	110° nominal
Elevation-Plane Beamwidth: (Half-Power Points)	30° nominal
Elevation Angle of Maximum Radiation:	Depends on soil characteristics (0° over perfect earth)
Impedance:	50 ohms
Transmission-Line Connector:	50 ohm, 1-5/8" EIA flange
Power Handling Capability:	20 kw peak, 10 kw average
Tower Height:	140 feet
Site Area Requirement:	430 x 420 feet (typical)
Environment:	120 knots, no ice; 50 knots, 1-1/2 inch radial ice.

Figure 5. Characteristics of the 726-2.5/30-T Antenna

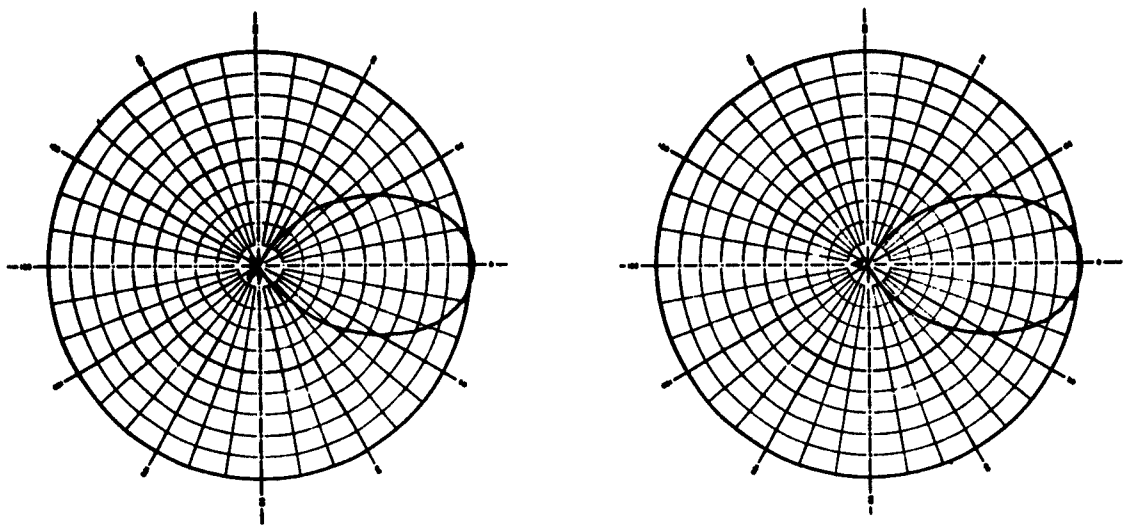

3.0 Mc 3.38 Mc

AZIMUTH PLANE

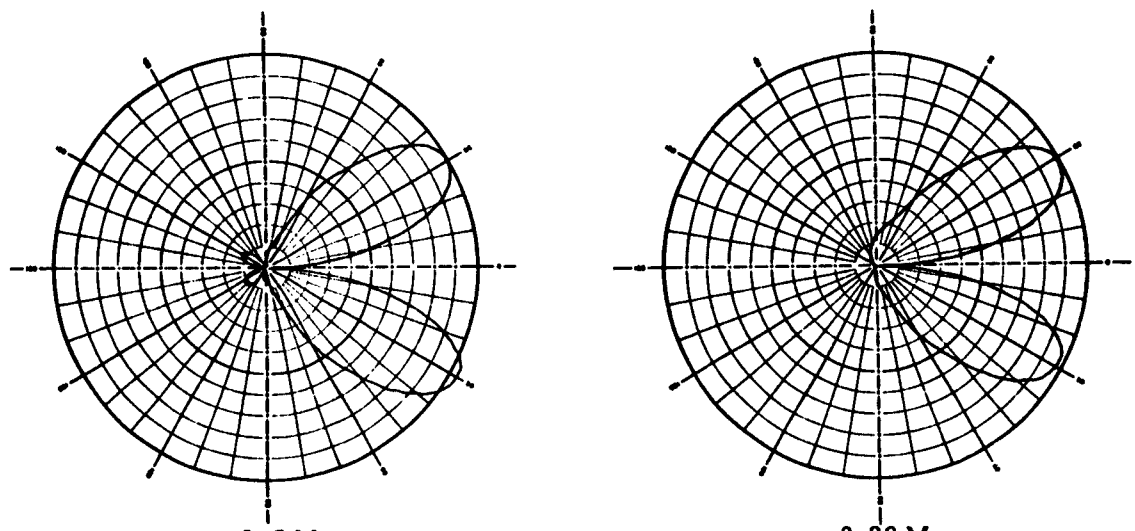

3.0 Mc 3.38 Mc

VERTICAL PLANE

Figure 6. Model Radiation Patterns, 748-3/30-15N Antenna, (imaged).

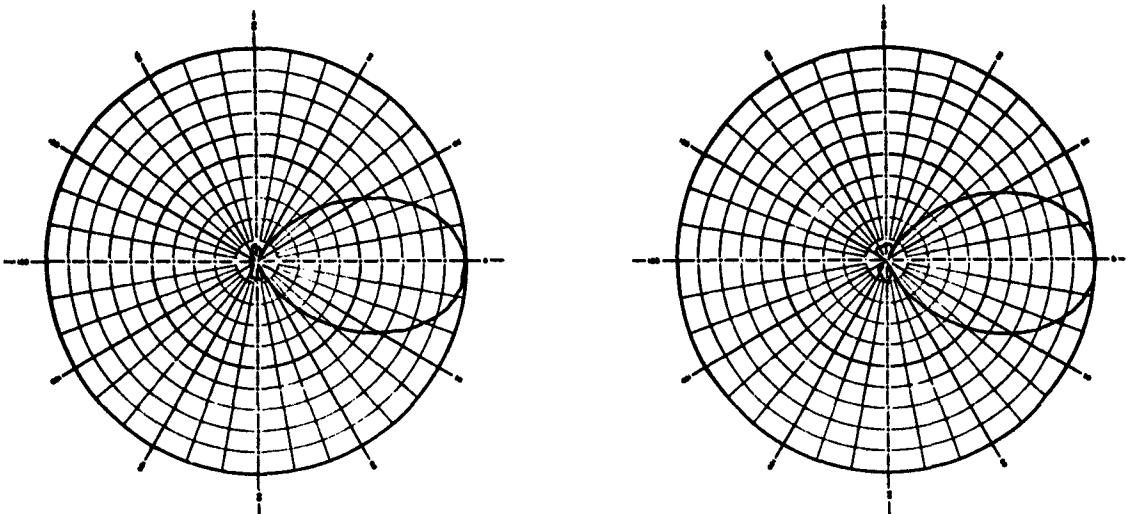

3.8 Mc 4.23 Mc

AZIMUTH PLANE

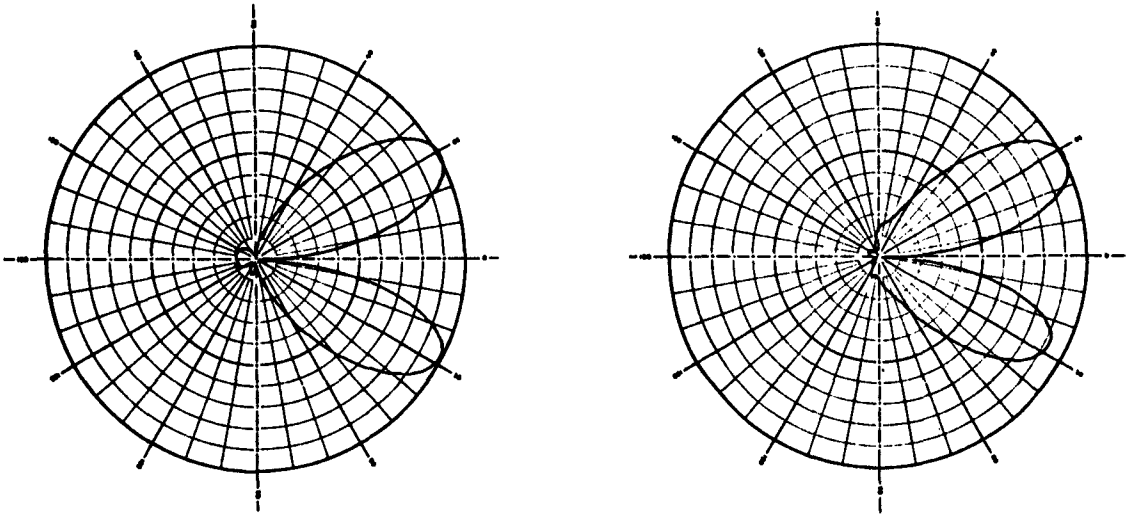

3.8 Mc 4.23 Mc

VERTICAL PLANE

Figure 6-A. Model Radiation Patterns, 748-3/30-15N Antenna, (imaged).

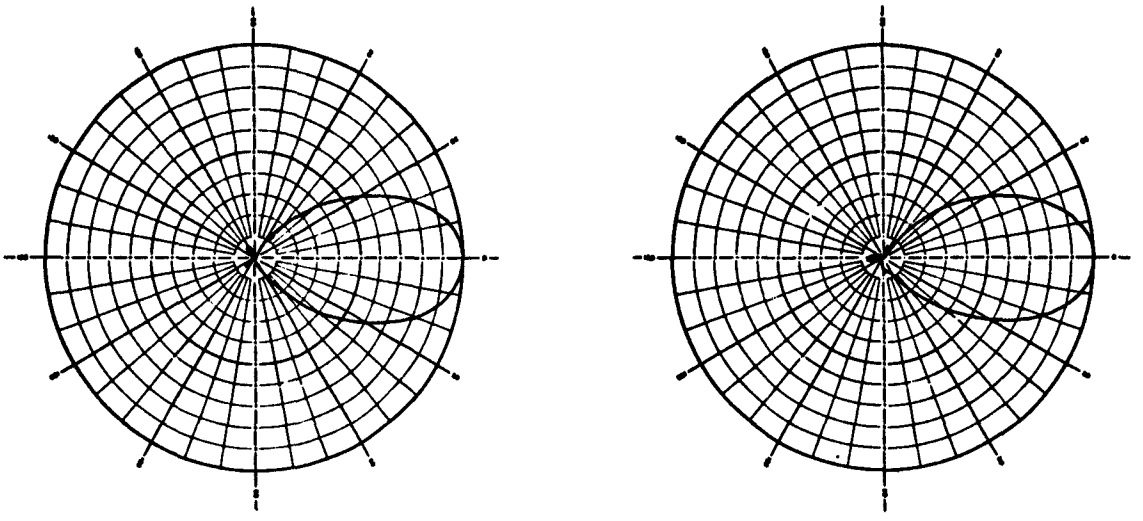

4.65 Mc 5.07 Mc

AZIMUTH PLANE

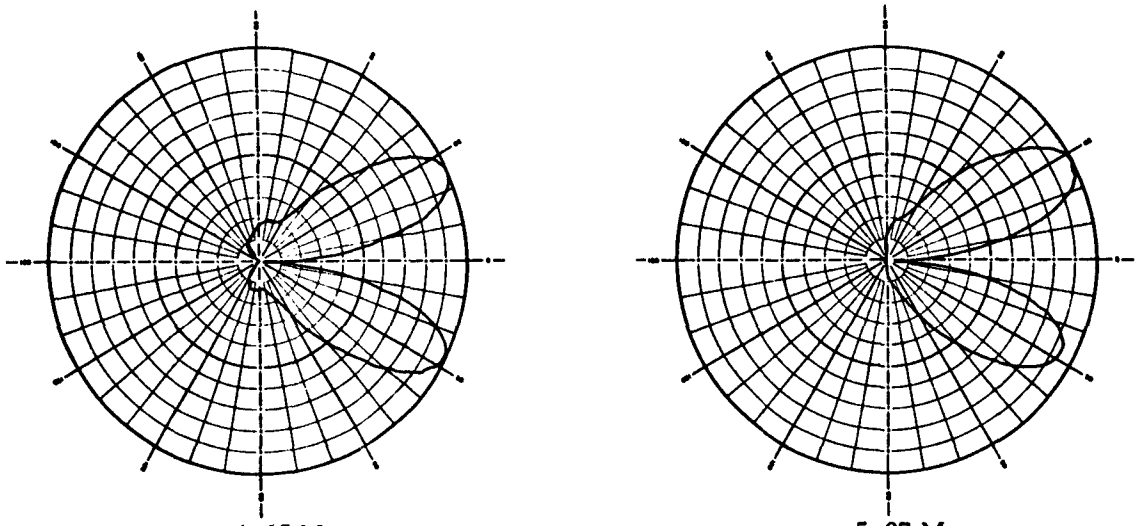

4.65 Mc 5.07 Mc

VERTICAL PLANE

Figure 6-B. Model Radiation Patterns, 748-3/30-15N Antenna, (imaged).

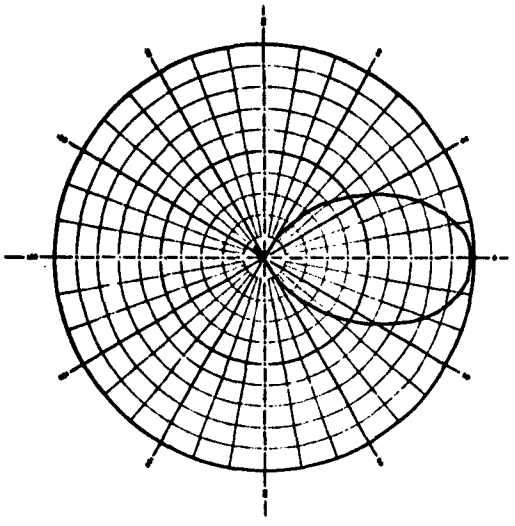

5.49 Mc

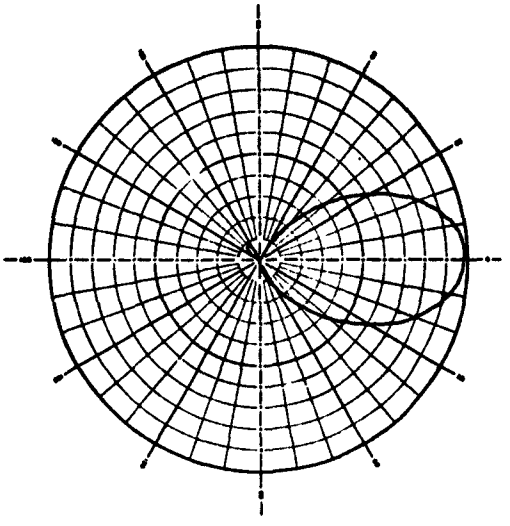

5.92 Mc

AZIMUTH PLANE

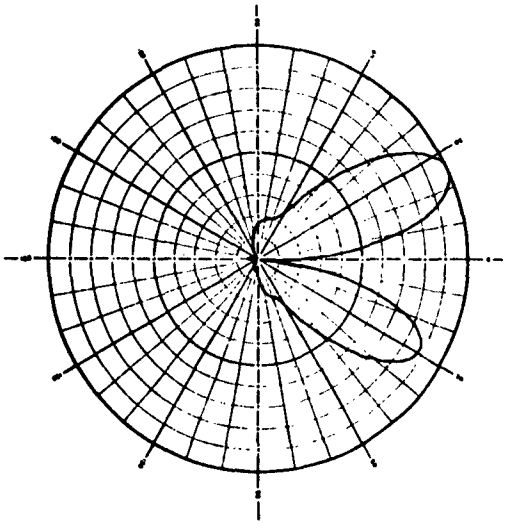

5.49 Mc

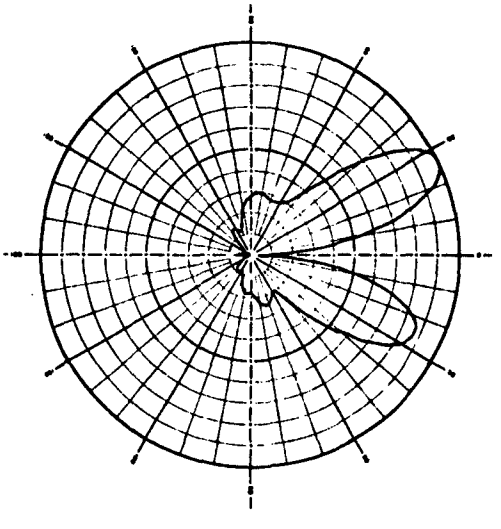

5.92 Mc

VERTICAL PLANE

Figure 6-C. Model Radiation Patterns, 748-3/30-15N Antenna, (imaged).

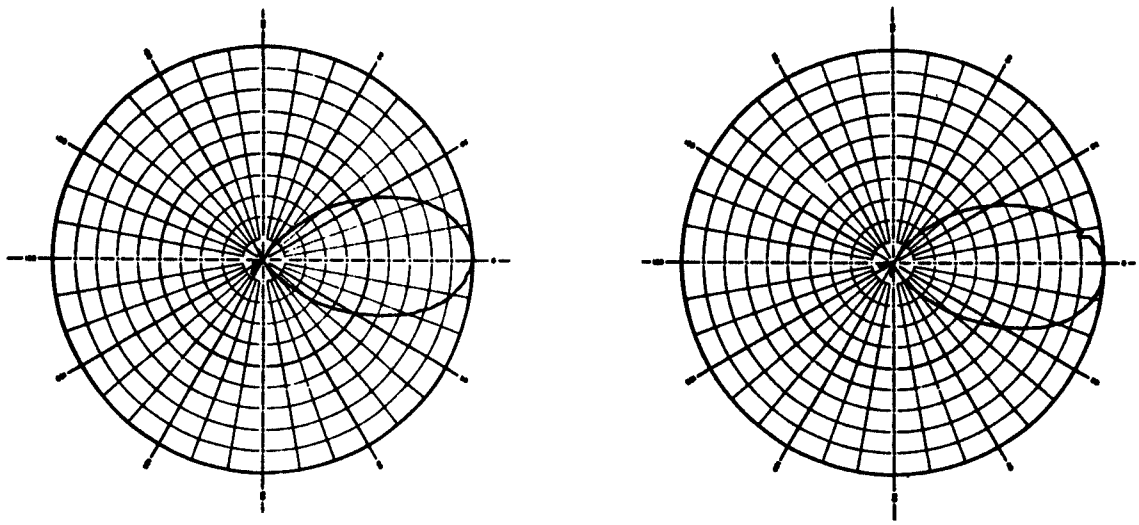

6.34 Mc 6.76 Mc

AZIMUTH PLANE

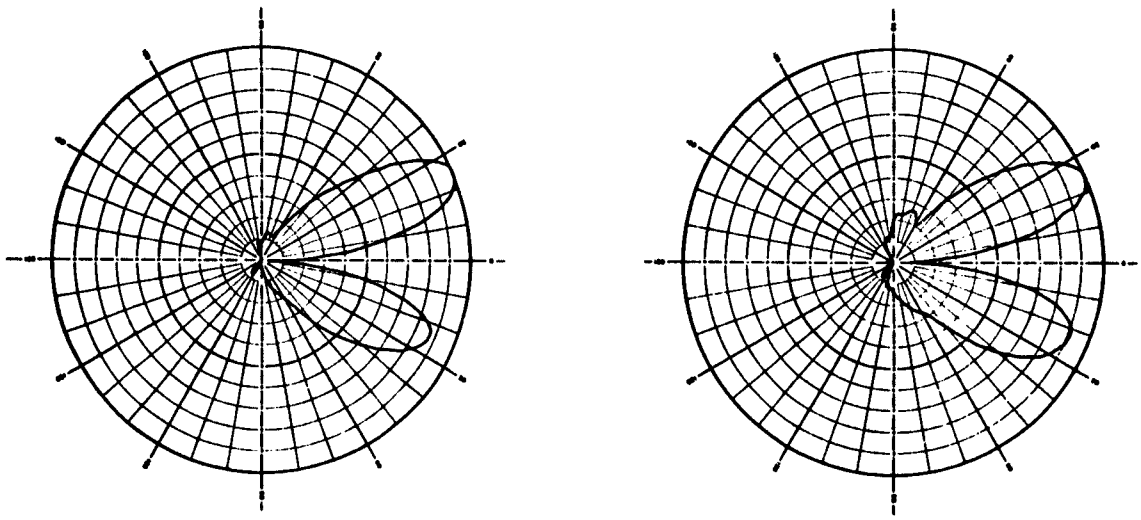

6.34 Mc 6.76 Mc

VERTICAL PLANE

Figure 6-D. Model Radiation Patterns, 748-3/30-15N Antenna, (imaged).

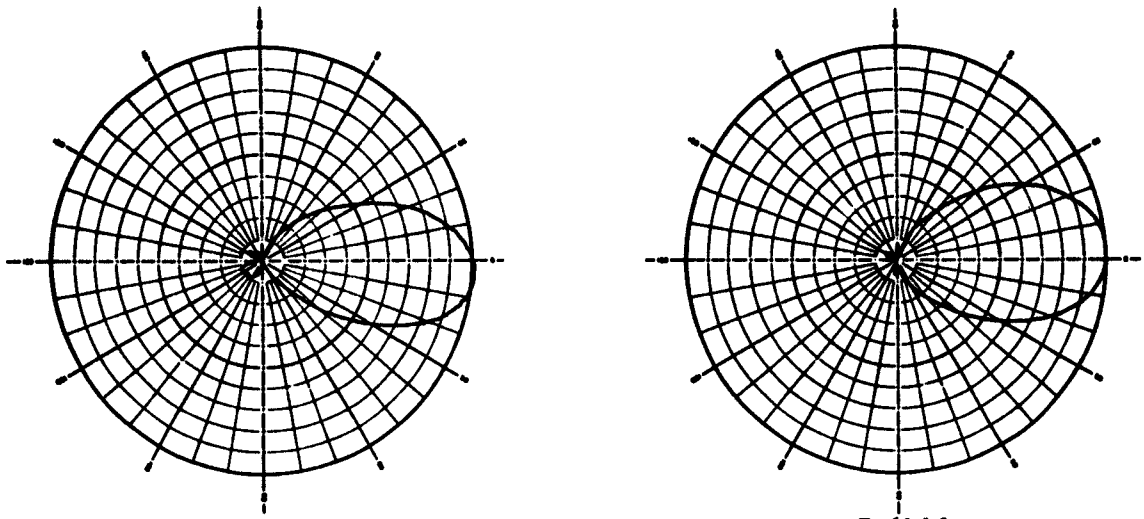

7.18 Mc 7.61 Mc

AZIMUTH PLANE

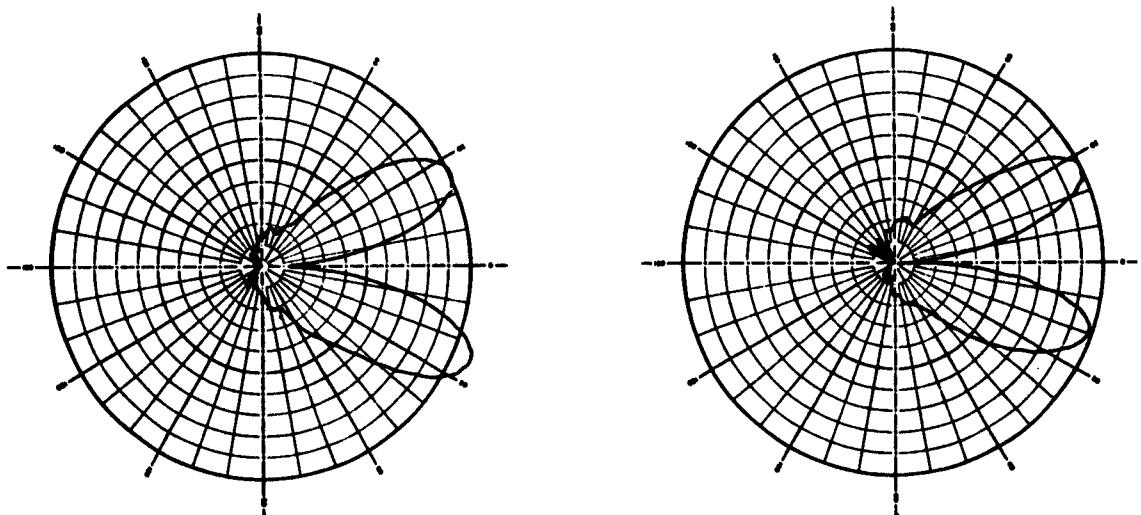

7.18 Mc 7.61 Mc

VERTICAL PLANE

Figure 6-E. Model Radiation Patterns, 748-3/30-15N Antenna, (imaged).

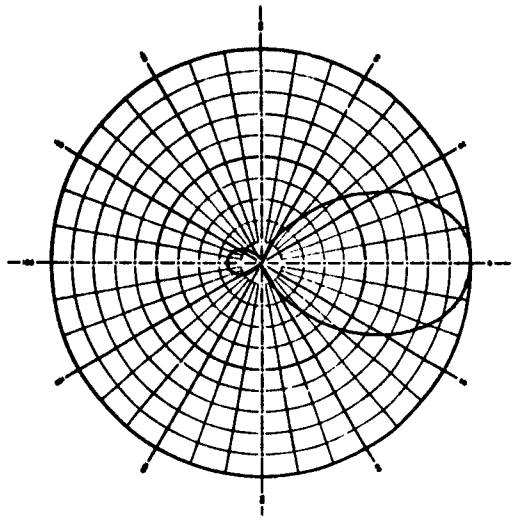

13.1 Mc

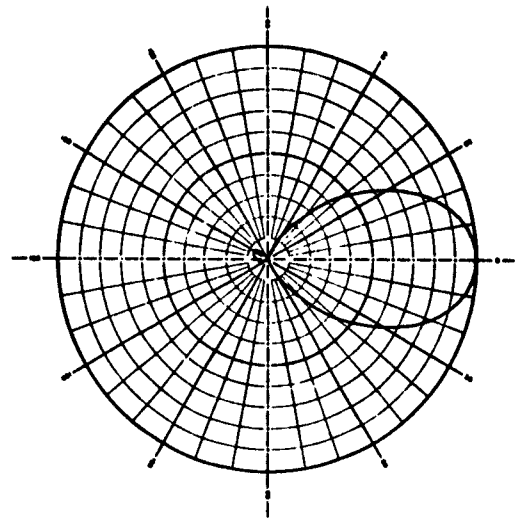

14.77 Mc

AZIMUTH PLANE

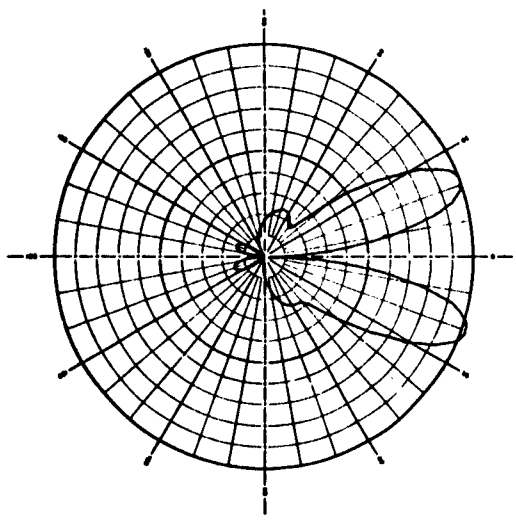

13.1 Mc

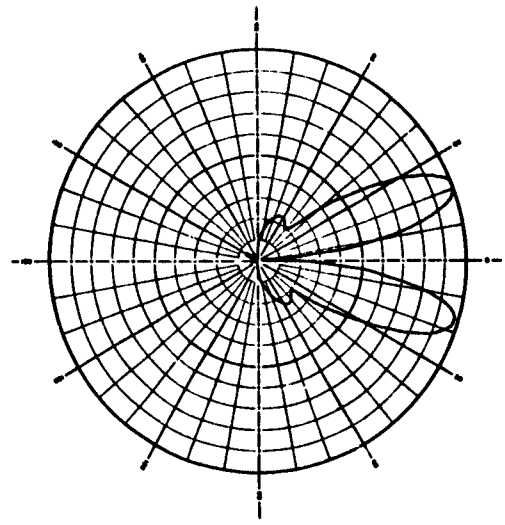

14.77 Mc

VERTICAL PLANE

Figure 6-F. Model Radiation Patterns, 748-3/30-15N Antenna, (imaged).

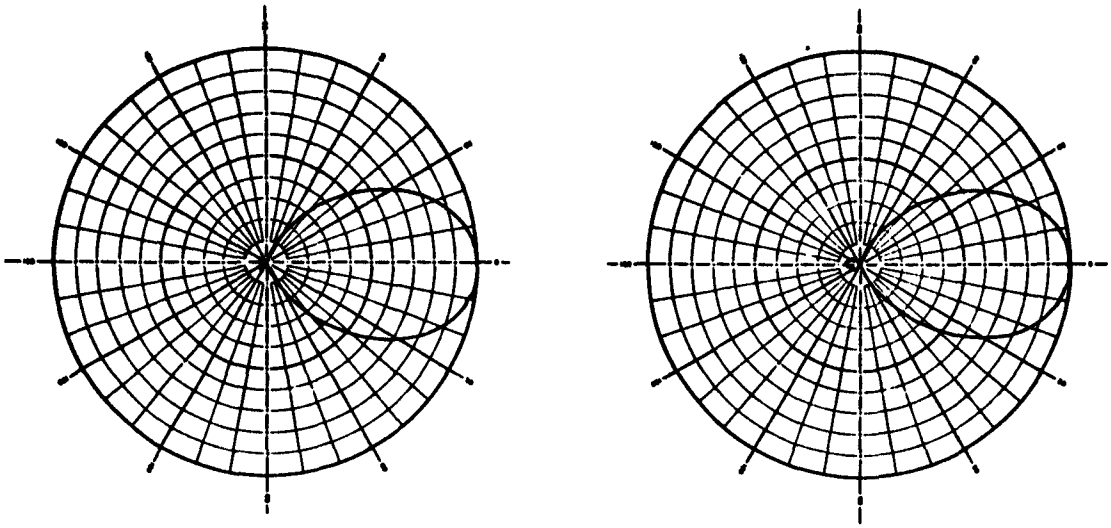

16.6 Mc 18.47 Mc

AZIMUTH PLANE

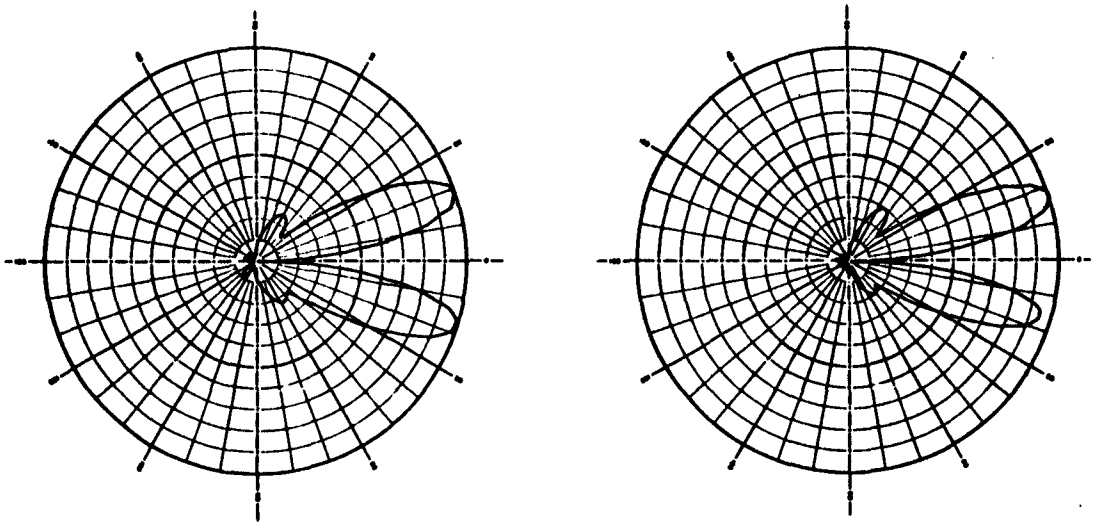

16.6 Mc 18.47 Mc

VERTICAL PLANE

Figure 6-G. Model Radiation Patterns, 748-3/30-15N Antenna, (imaged).

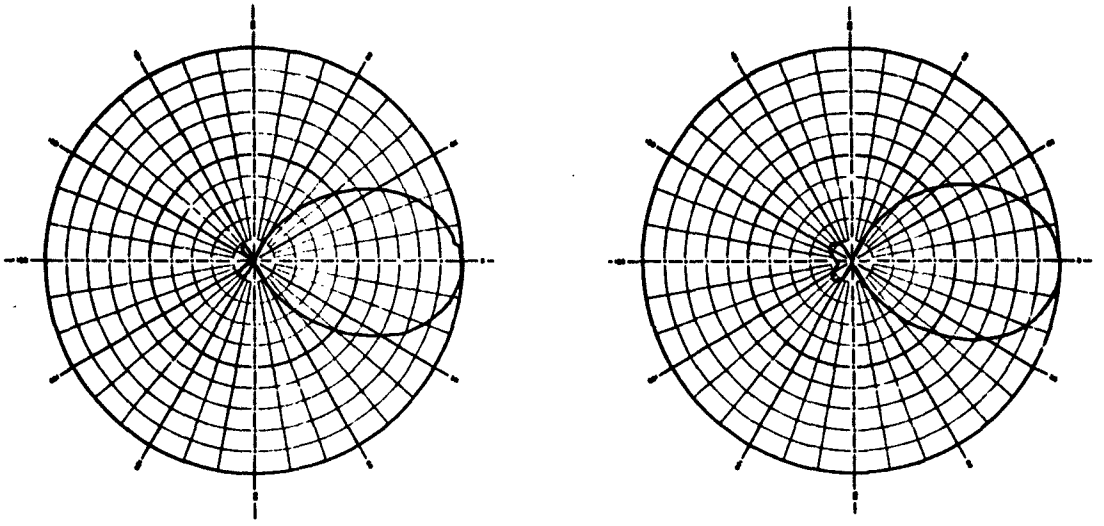

20.3 Mc 22.15 Mc

AZIMUTH PLANE

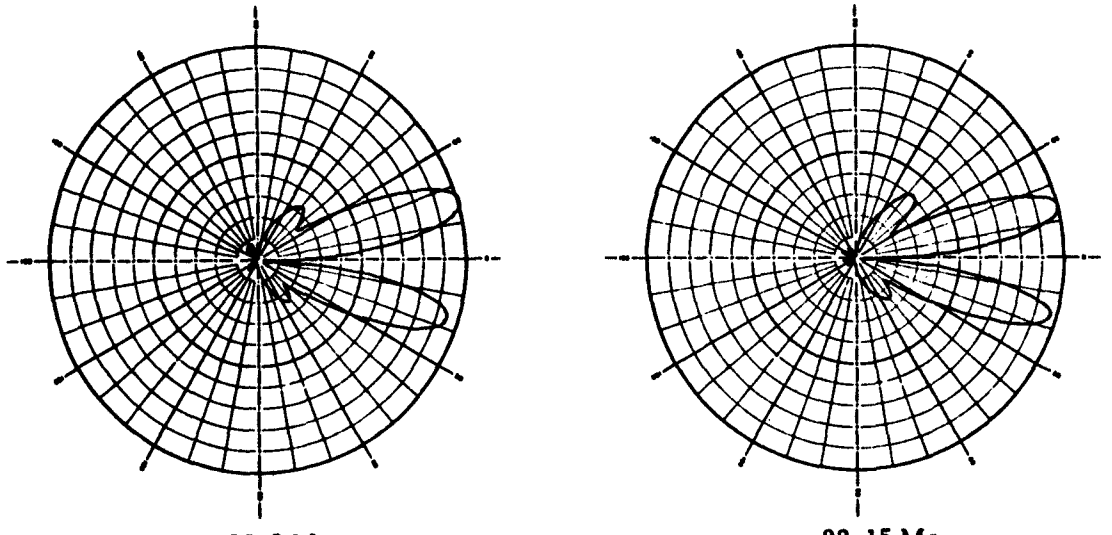

20.3 Mc 22.15 Mc

VERTICAL PLANE

Figure 6-H. Model Radiation Patterns, 748-3/30-15N Antenna, (imaged).

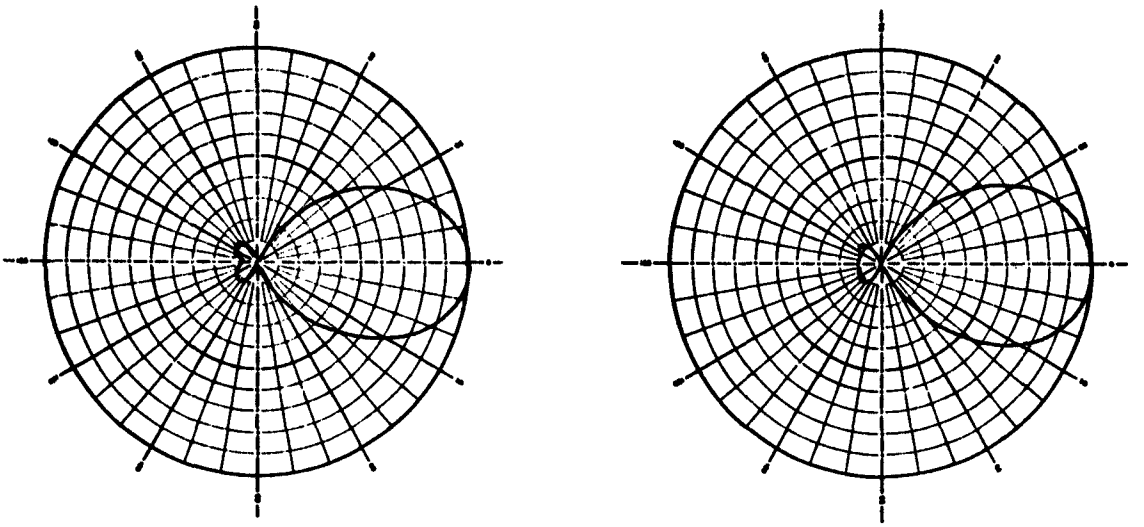

24 Mc 25.8 Mc

AZIMUTH PLANE

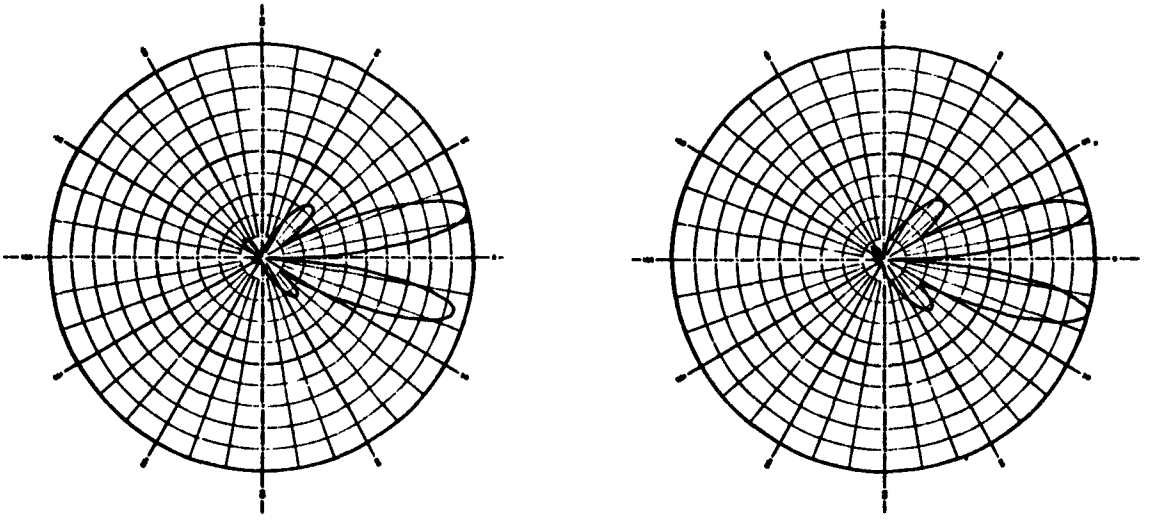

24 Mc 25.8 Mc

VERTICAL PLANE

Figure 6-I. Model Radiation Patterns, 748-3/30-15N Antenna, (imaged).

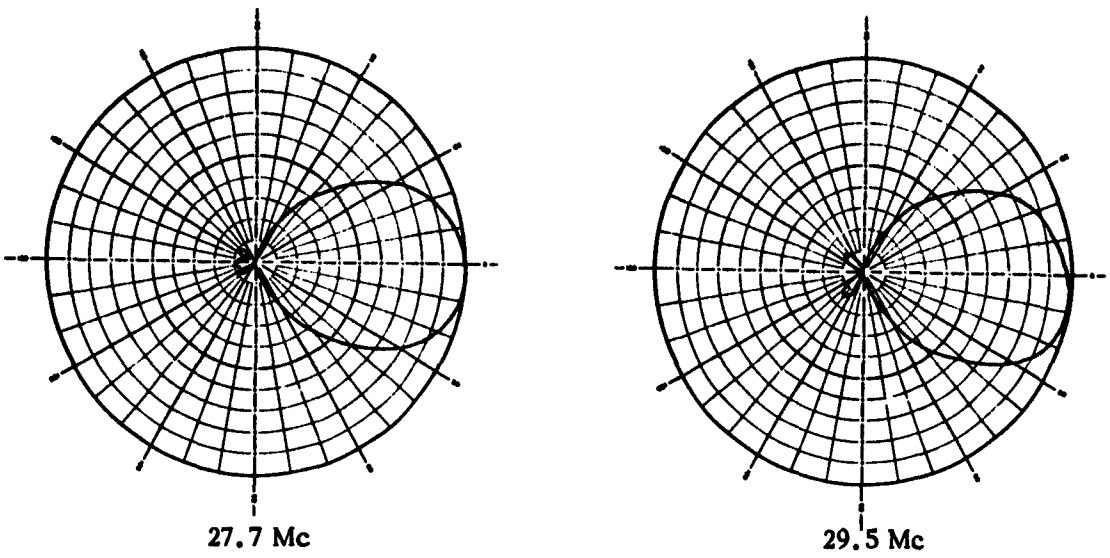

27.7 Mc 29.5 Mc

AZIMUTH PLANE

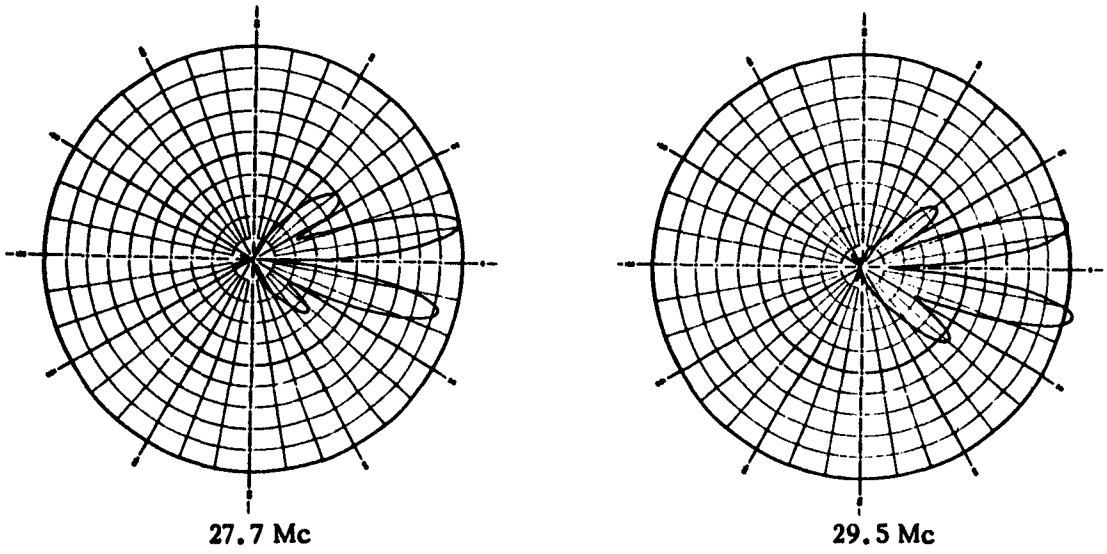

27.7 Mc 29.5 Mc

VERTICAL PLANE

Figure 6-J. Model Radiation Patterns, 748-3/30-15N Antenna, (imaged).

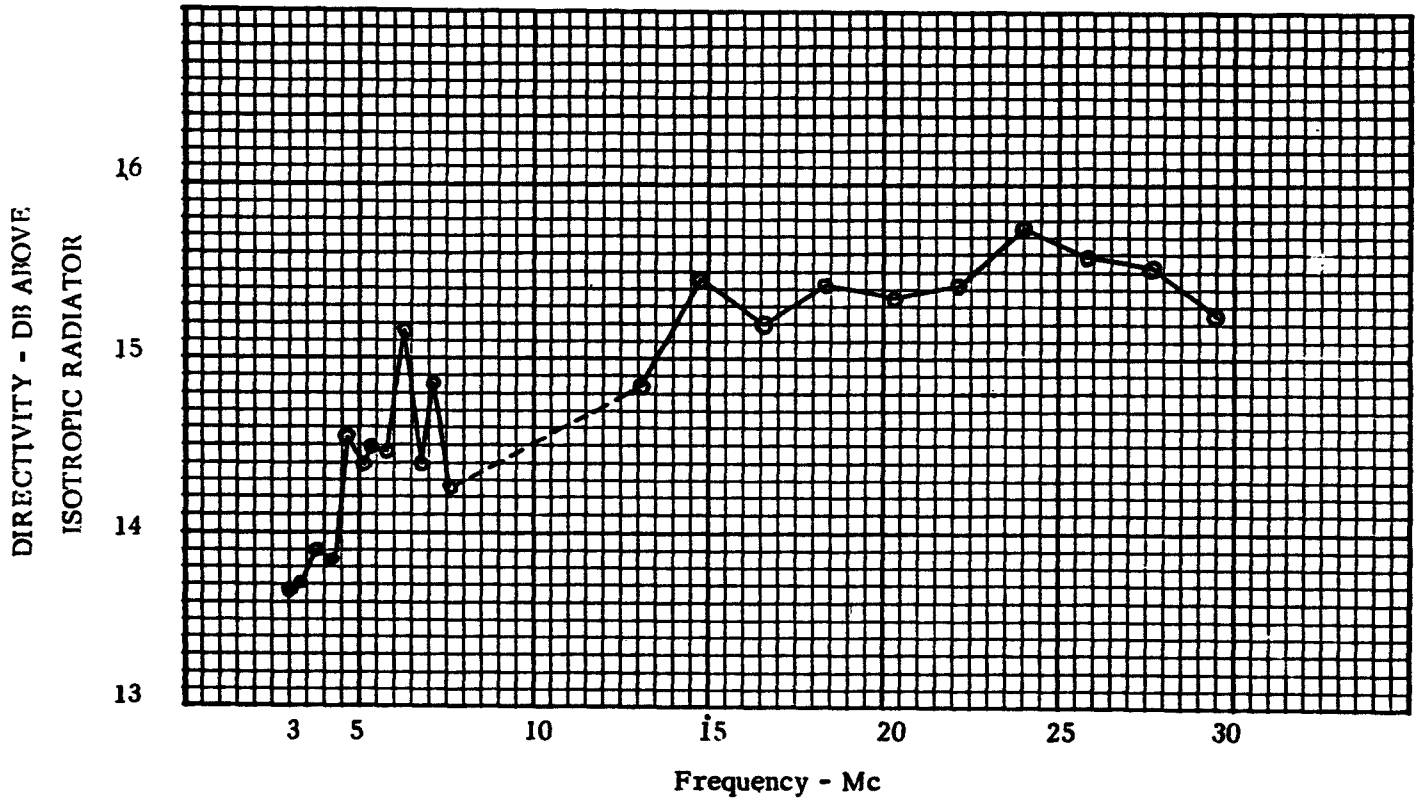

Figure 7. Directivity of 748-3/30-15N Antenna.

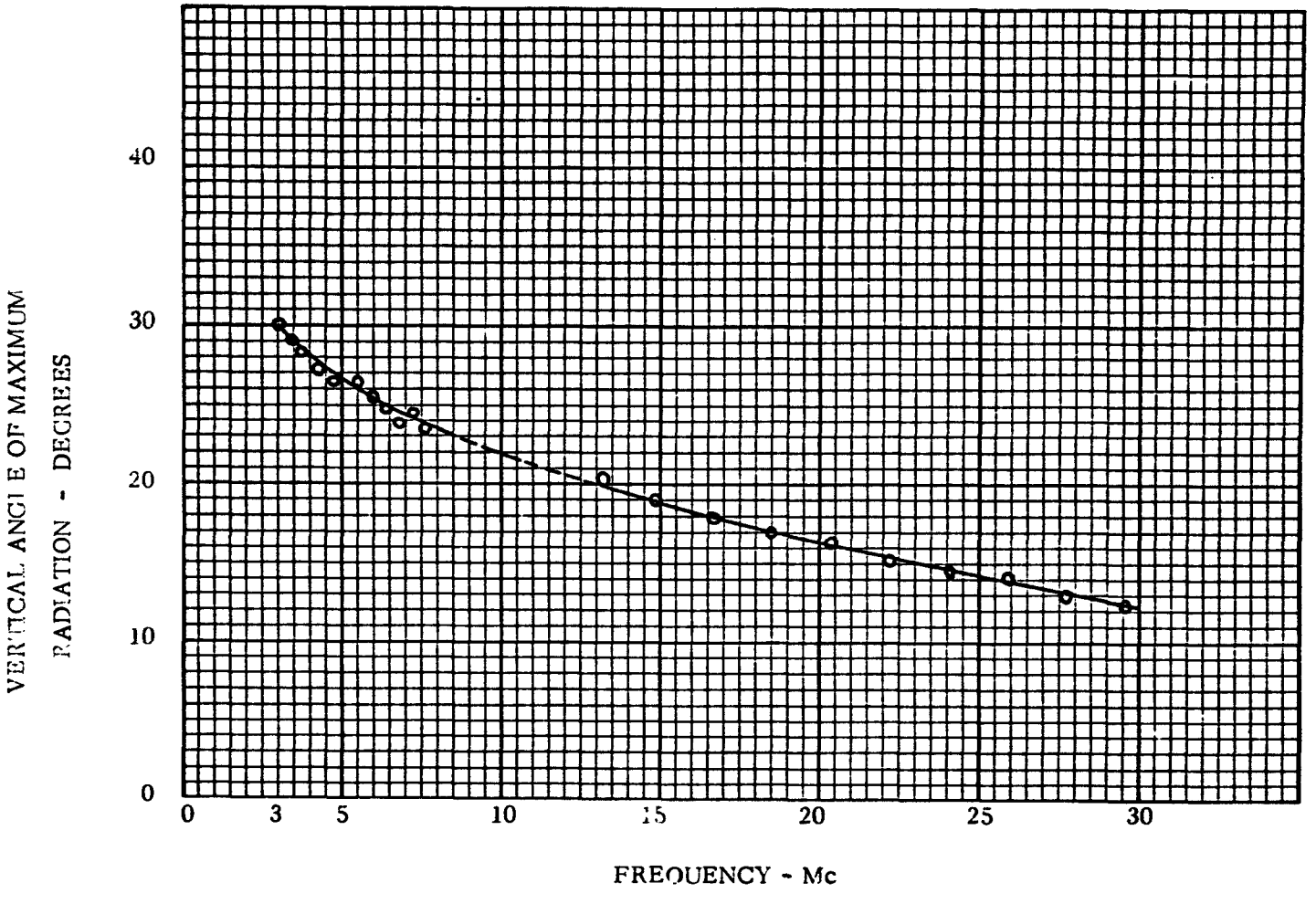

Figure 8. Elevation Angle of Maximum Radiation 748-3/30-15N Antenna

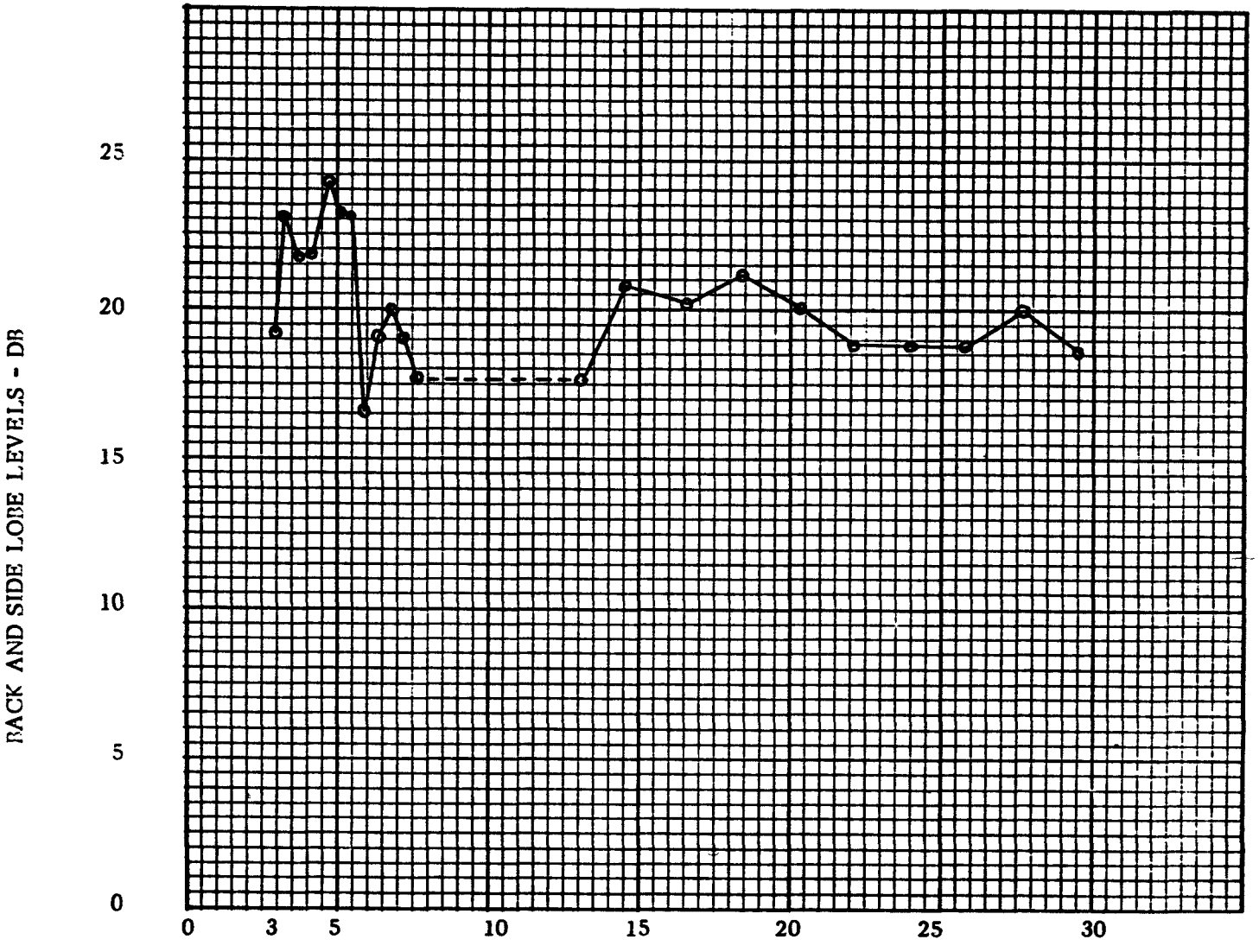

Figure 9. Back and Side Lobe Levels Type 748-3/30-15N Antenna

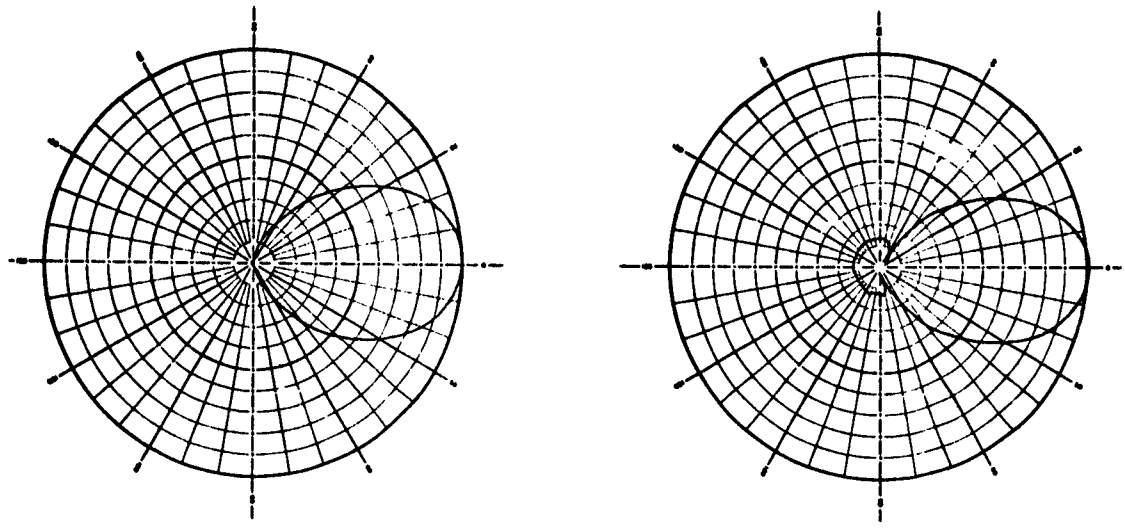

3.0 Mc 3.38 Mc

AZIMUTH PLANE

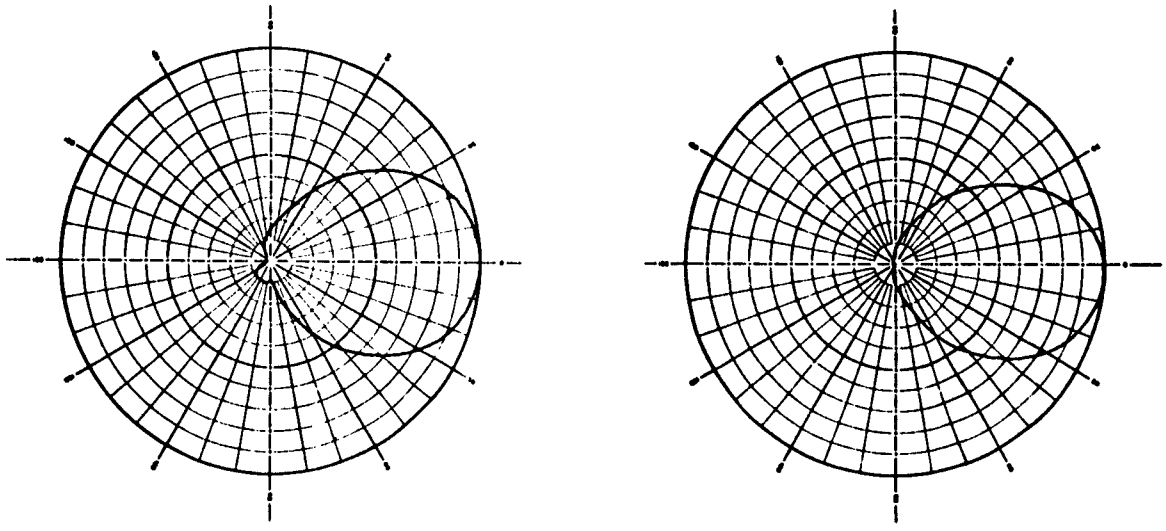

3.0 Mc 3.38 Mc

VERTICAL PLANE

Figure 10. Model Radiation Patterns, 748-3/30-15N Antenna. (Free-Space).

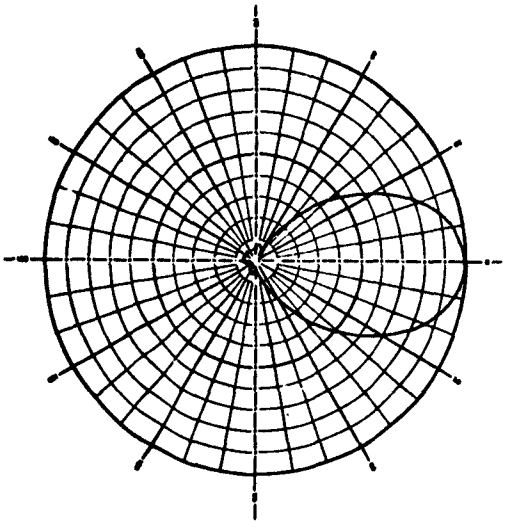

3.41 Mc

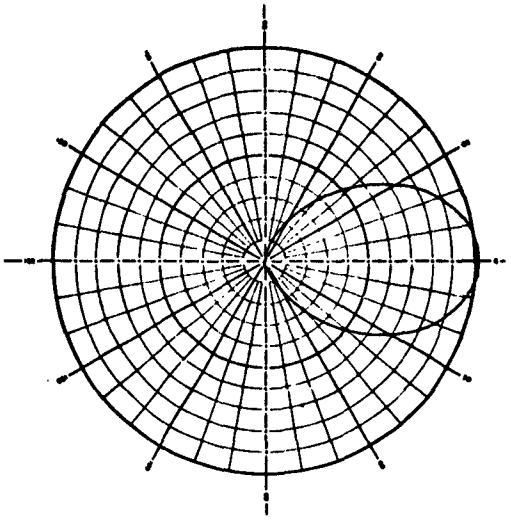

3.8 Mc

AZIMUTH PLANE

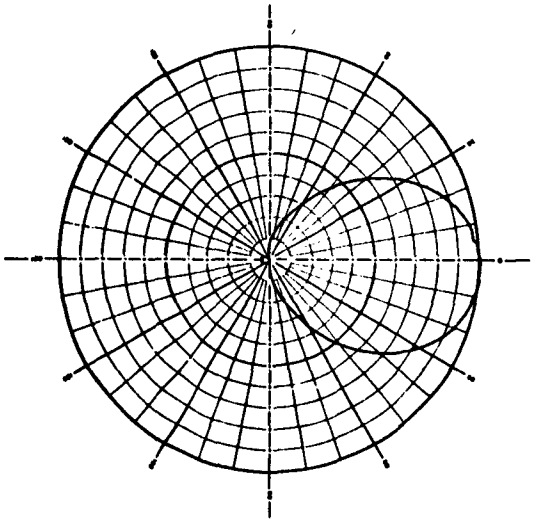

3.41 Mc

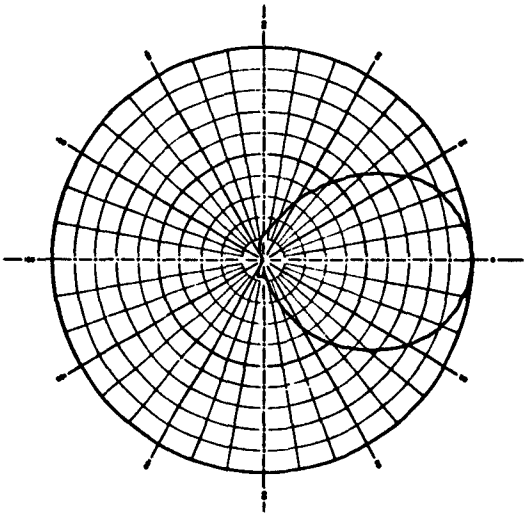

3.8 Mc

VERTICAL PLANE

Figure 10-A. Model Radiation Patterns, 748-3/30-15N Antenna. (Free-Space).

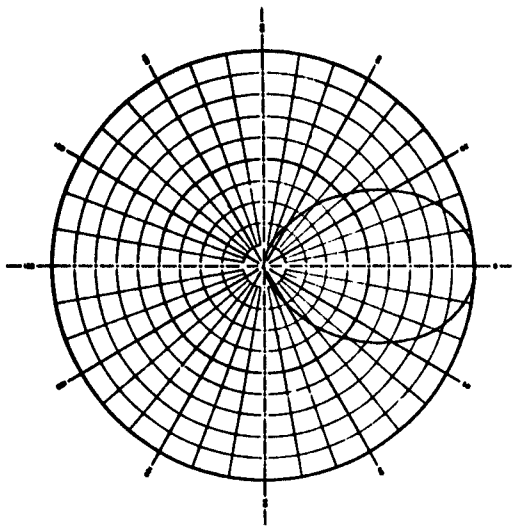

4.23 Mc

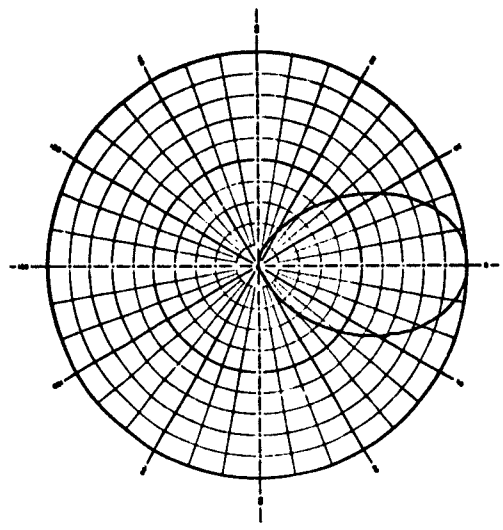

4.65 Mc

AZIMUTH PLANE

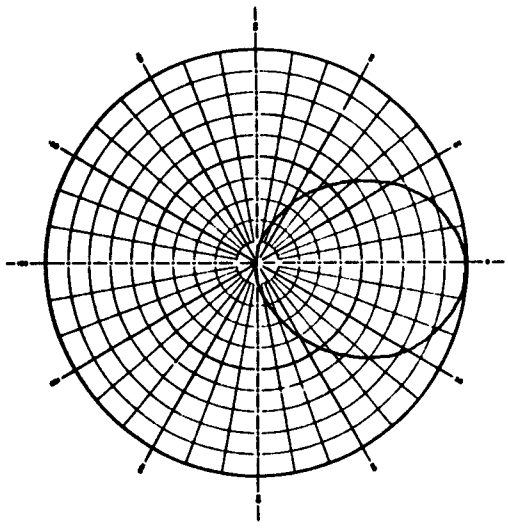

4.23 Mc

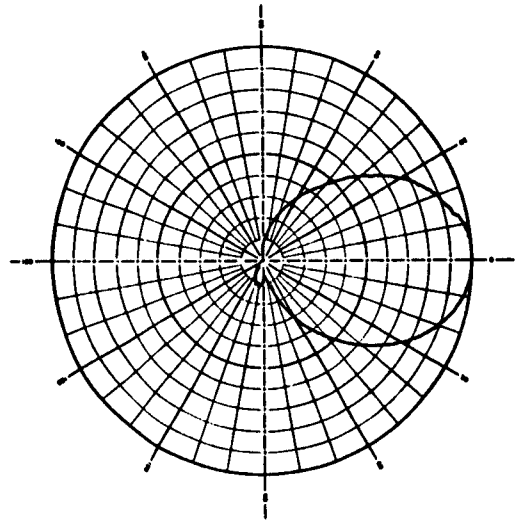

4.65 Mc

VERTICAL PLANE

Figure 10-B. Model Radiation Patterns, 748-3/30-15N Antenna. (Free-Space).

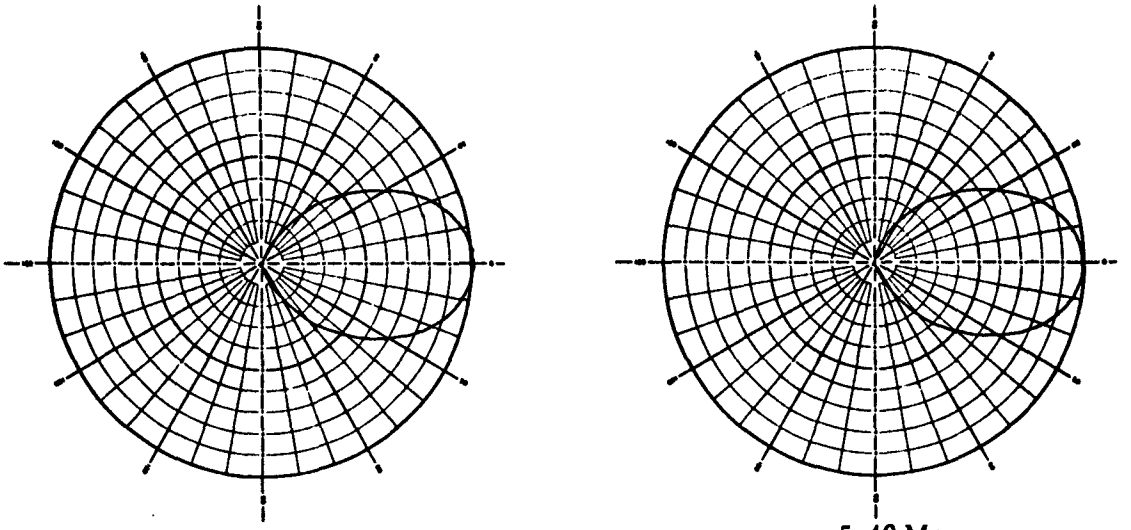

5.07 Mc 5.49 Mc

AZIMUTH PLANE

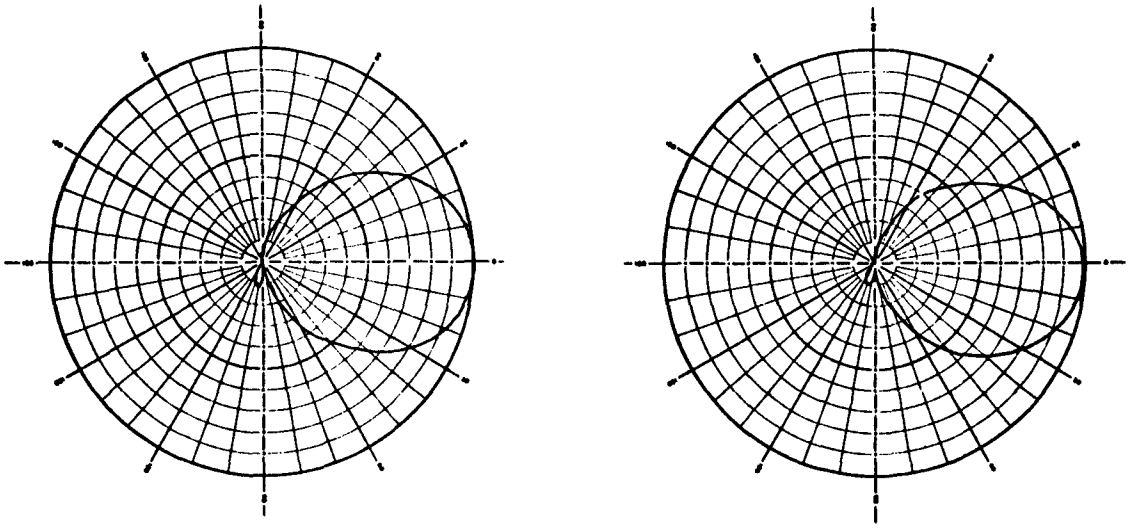

5.07 Mc 5.49 Mc

VERTICAL PLANE

Figure 10-C. Model Radiation Patterns, 748-3/30-15N Antenna. (Free-Space).

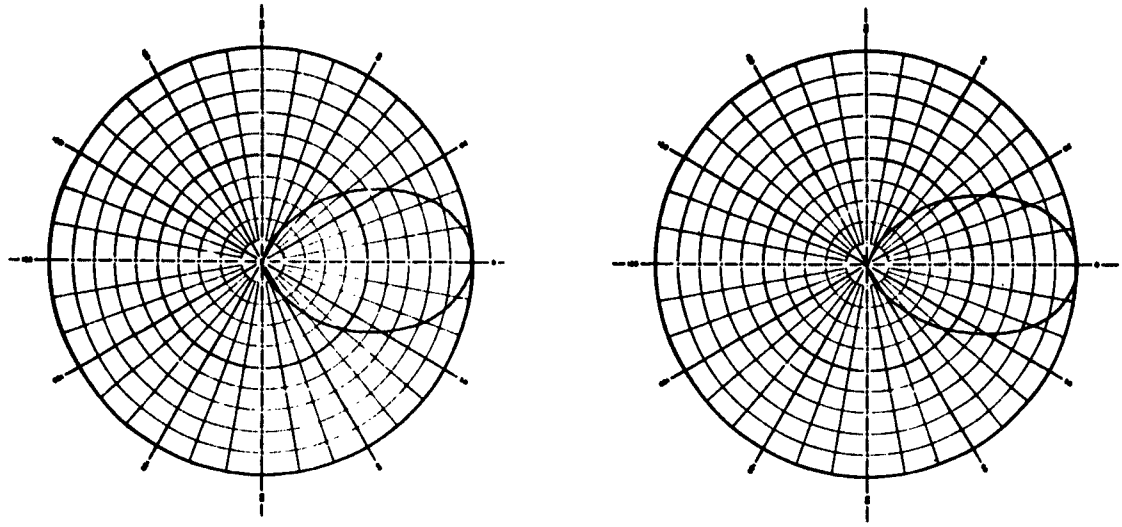

5.92 Mc 6.34 Mc

AZIMUTH PLANE

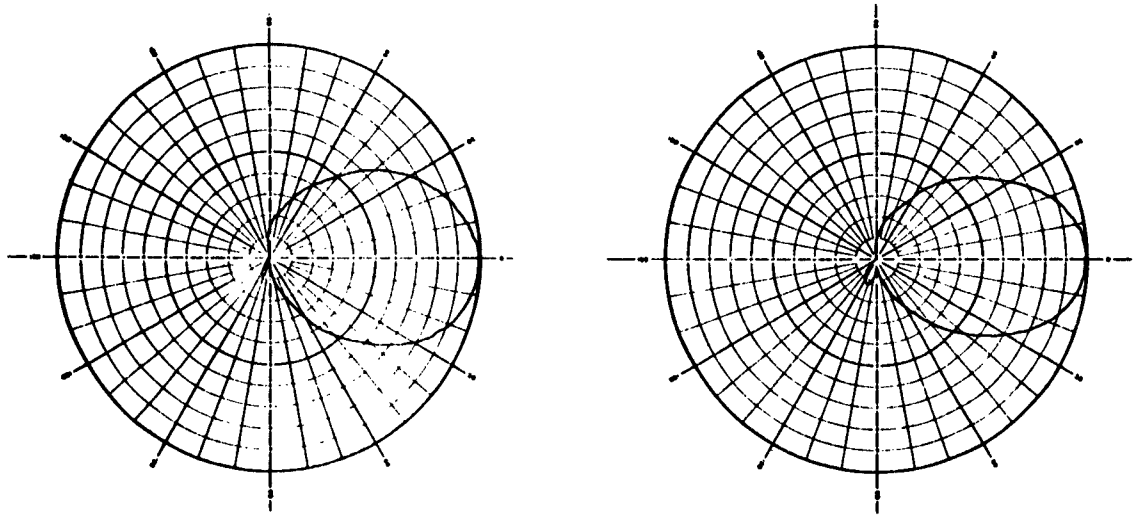

5.92 Mc 6.34 Mc

VERTICAL PLANE

Figure 10-D. Model Radiation Patterns, 748-3/30-15N Antenna. (Free-Space).

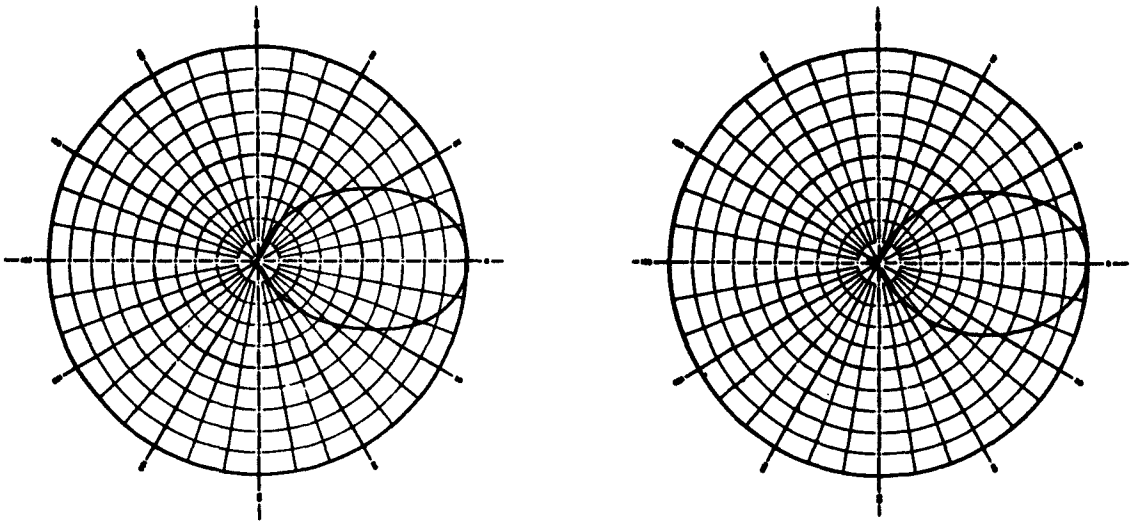

6.85 Mc 7.18 Mc

AZIMUTH PLANE

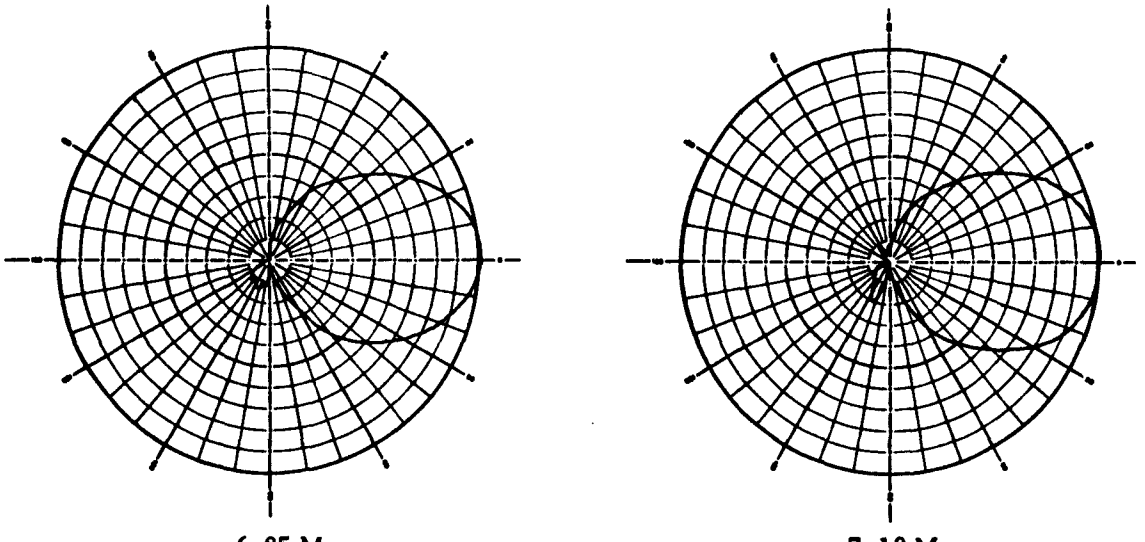

6.85 Mc 7.18 Mc

VERTICAL PLANE

Figure 10-E. Model Radiation Patterns, 748-3/30-15N Antenna. (Free-Space).

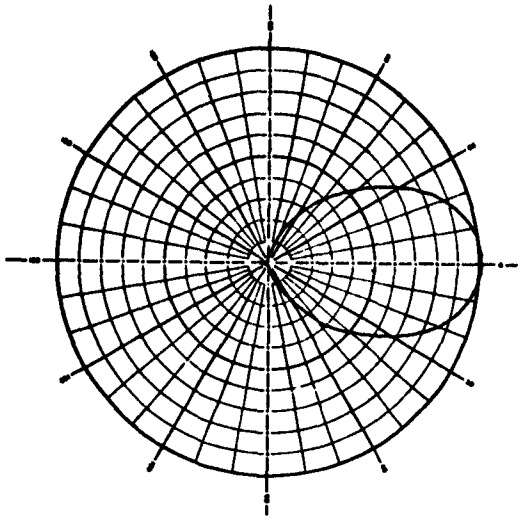

7.61 Mc

AZIMUTH PLANE

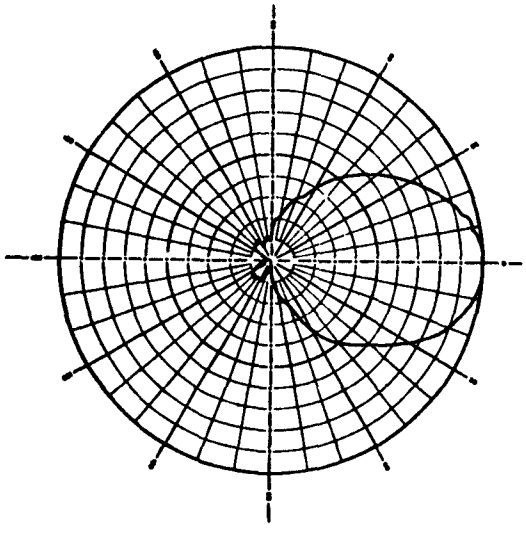

7.61 Mc

VERTICAL PLANE

Figure 10-F. Model Radiation Patterns, 748-3/30-15N Antenna. (Free-Space).

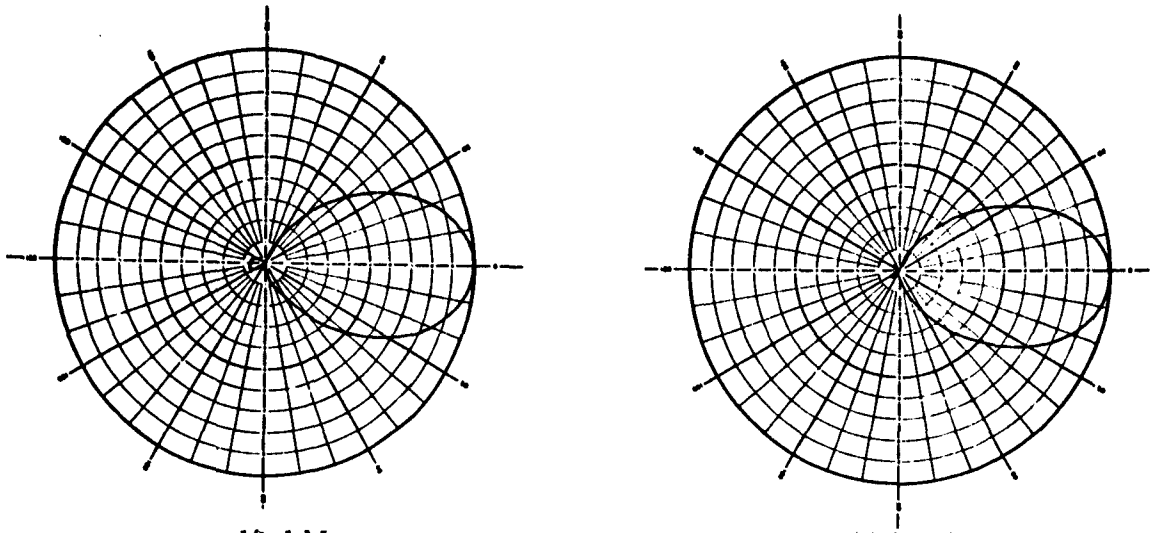

13.1 Mc 14.77 Mc

AZIMUTH PLANE

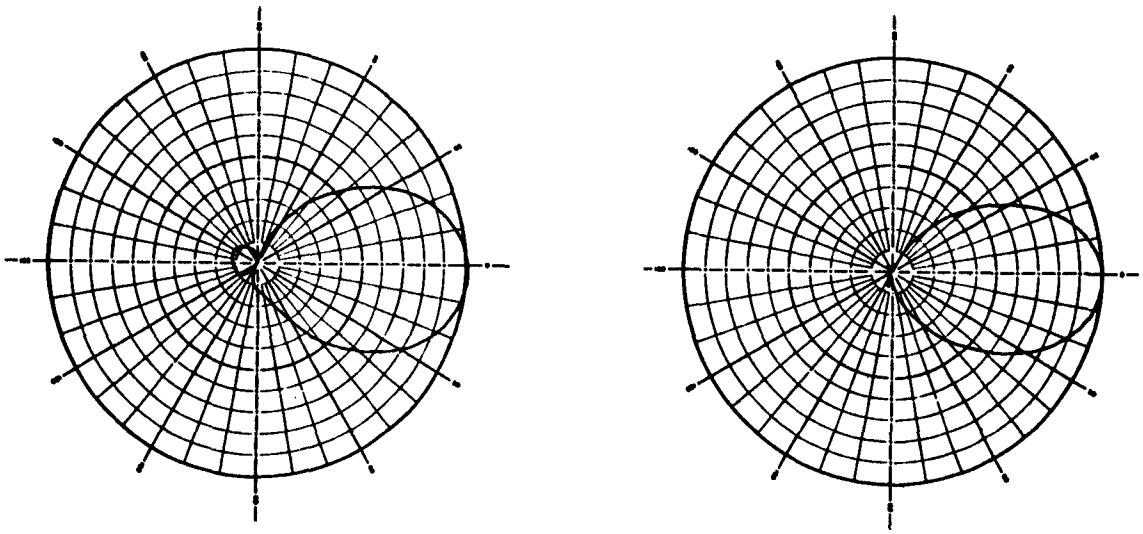

13.1 Mc 14.77 Mc

VERTICAL PLANE

Figure 10-G. Model Radiation Patterns, 748-3/30-15N Antenna. (Free-Space).

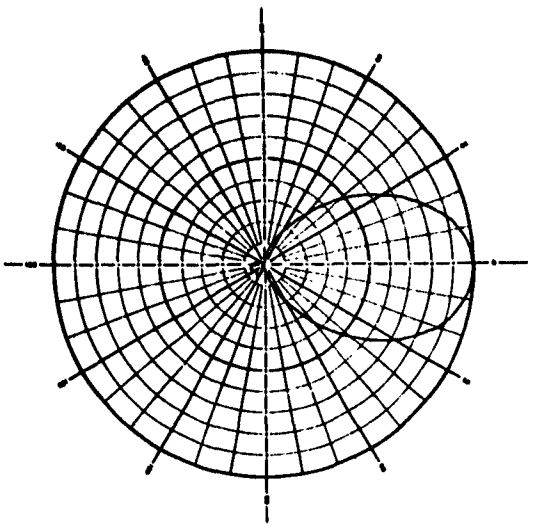

16.6 Mc

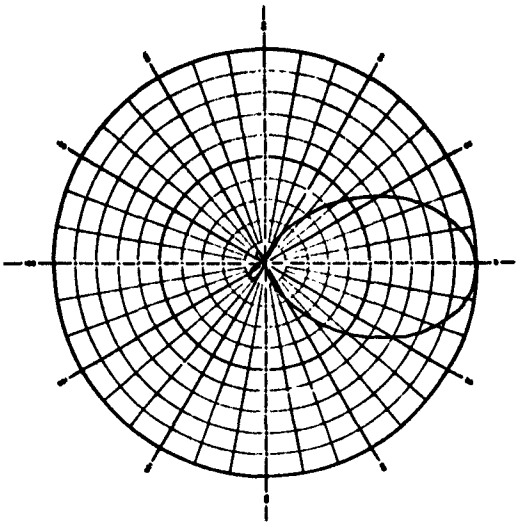

18.47

AZIMUTH PLANE

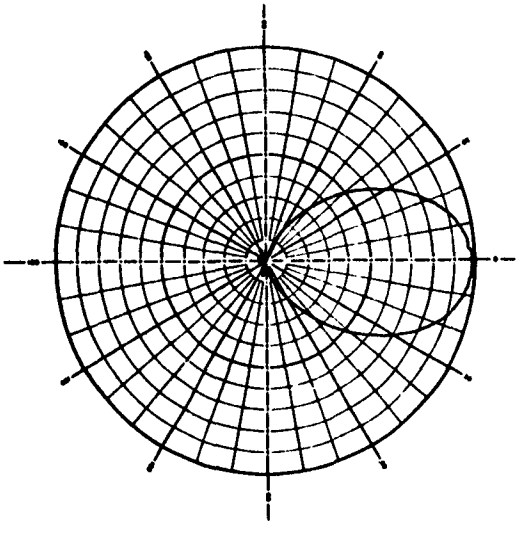

16.6 Mc

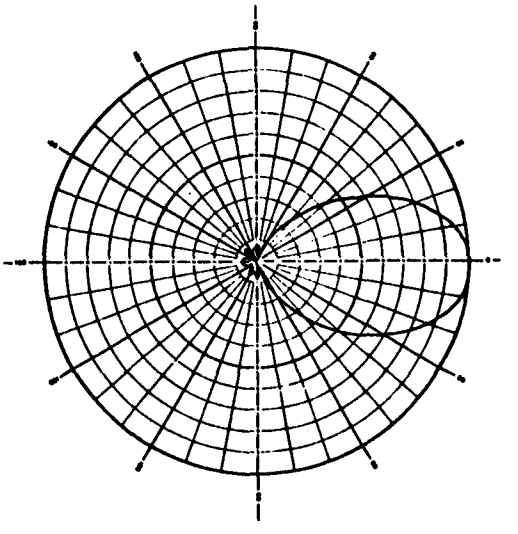

18.47 Mc

VERTICAL PLANE

Figure 10-H. Model Radiation Patterns, 748-3/30-15N Antenna. (Free-Space).

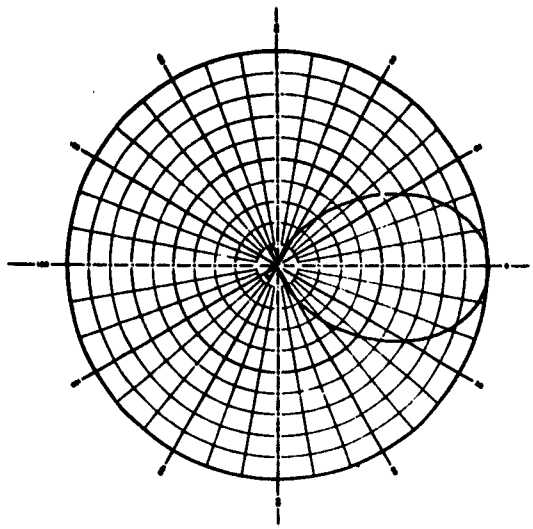

20.3 Mc

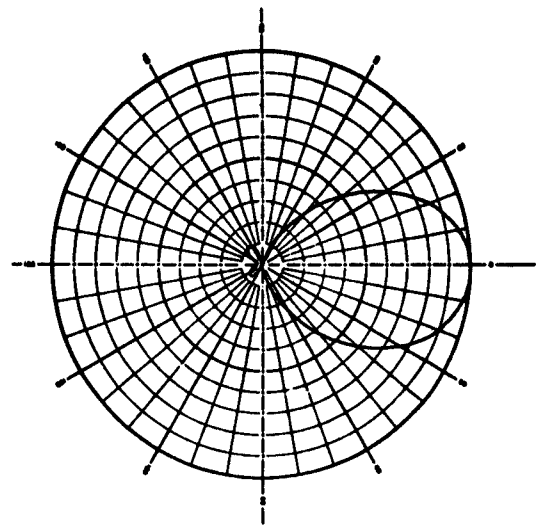

22.15 Mc

AZIMUTH PLANE

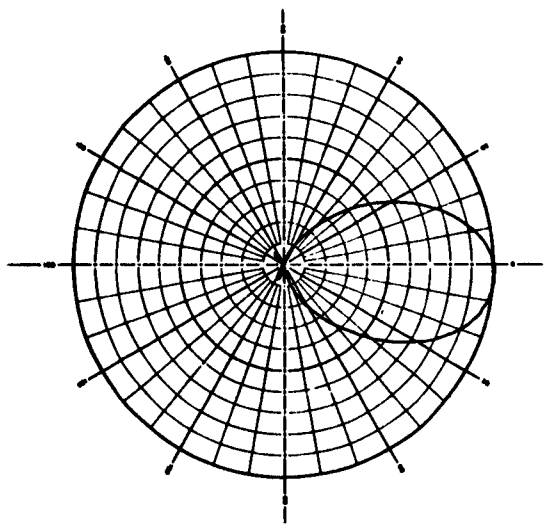

20.3 Mc

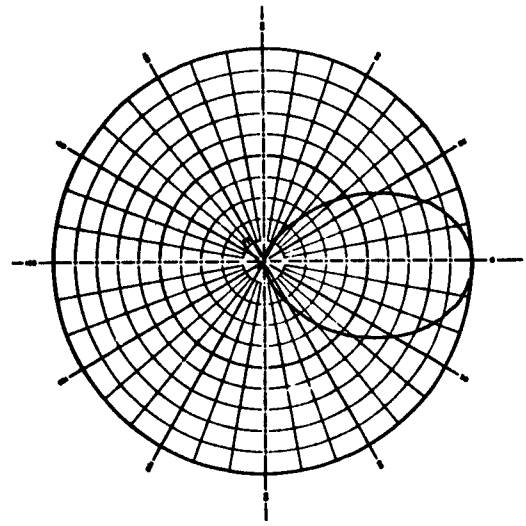

22.15 Mc

VERTICAL PLANE

Figure 10-I. Model Radiation Patterns, 748-3/30-15N Antenna. (Free-Space).

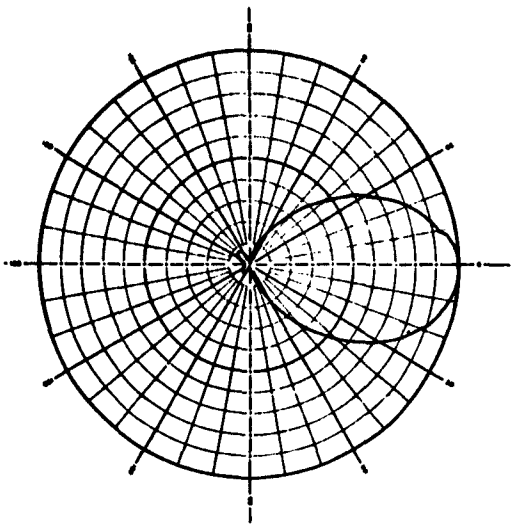

24 Mc

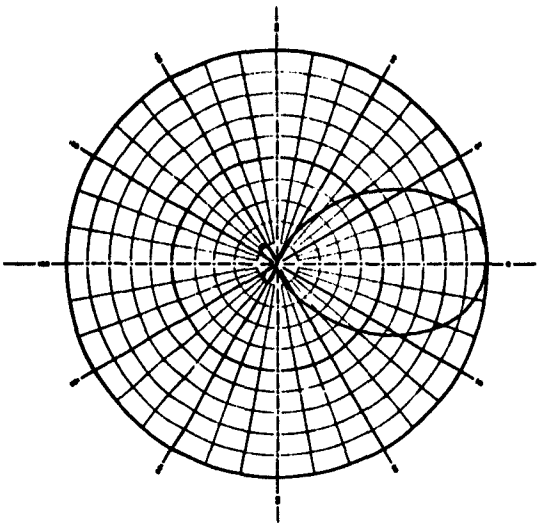

25.8 Mc

AZIMUTH PLANE

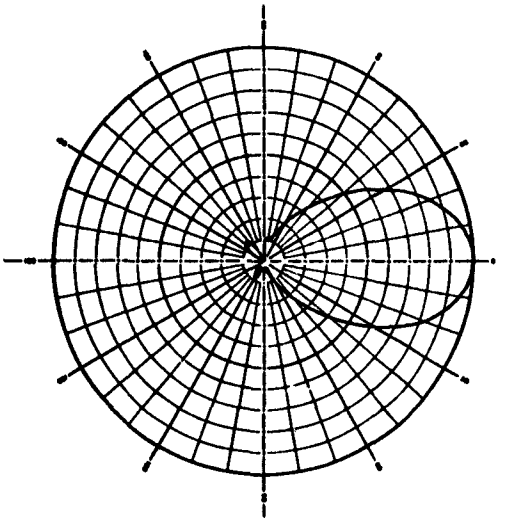

24 Mc

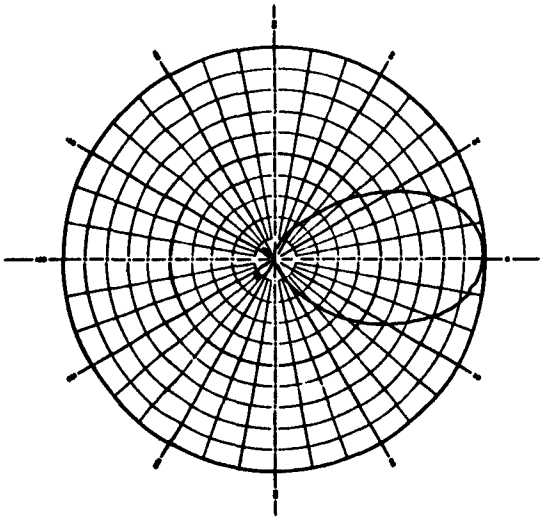

25.8 Mc

VERTICAL PLANE

Figure 10-J. Model Radiation Patterns, 748-3/30-15N Antenna. (Free-Space).

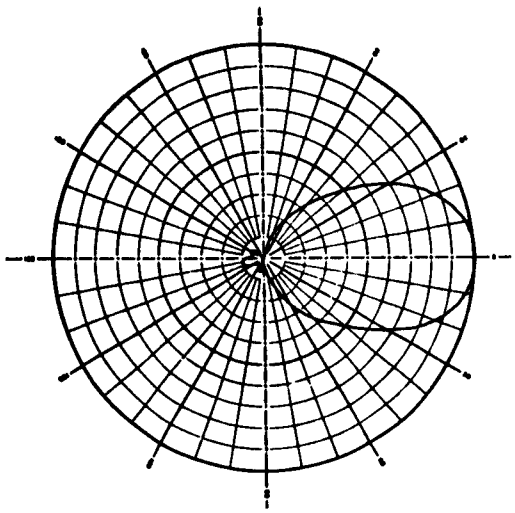

27.7 Mc

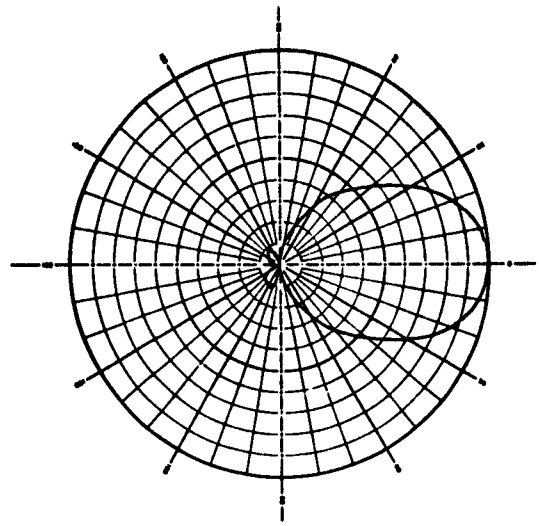

29.5 Mc

AZIMUTH PLANE

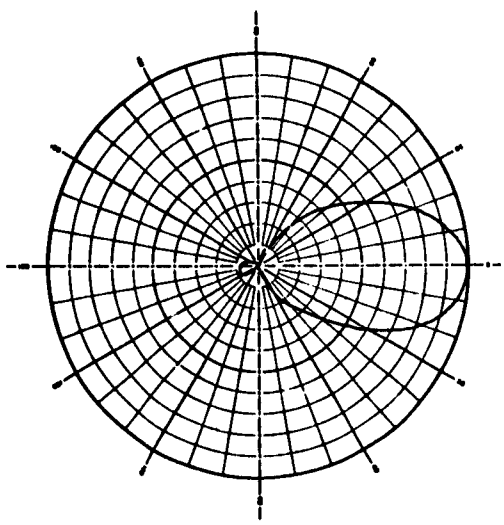

27.7 Mc

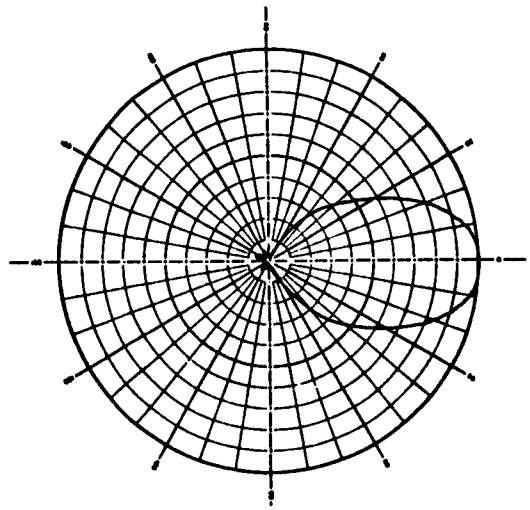

29.5 Mc

VERTICAL PLANE

Figure 10-K. Model Radiation Patterns, 748-3/30-15N Antenna. (Free-Space).

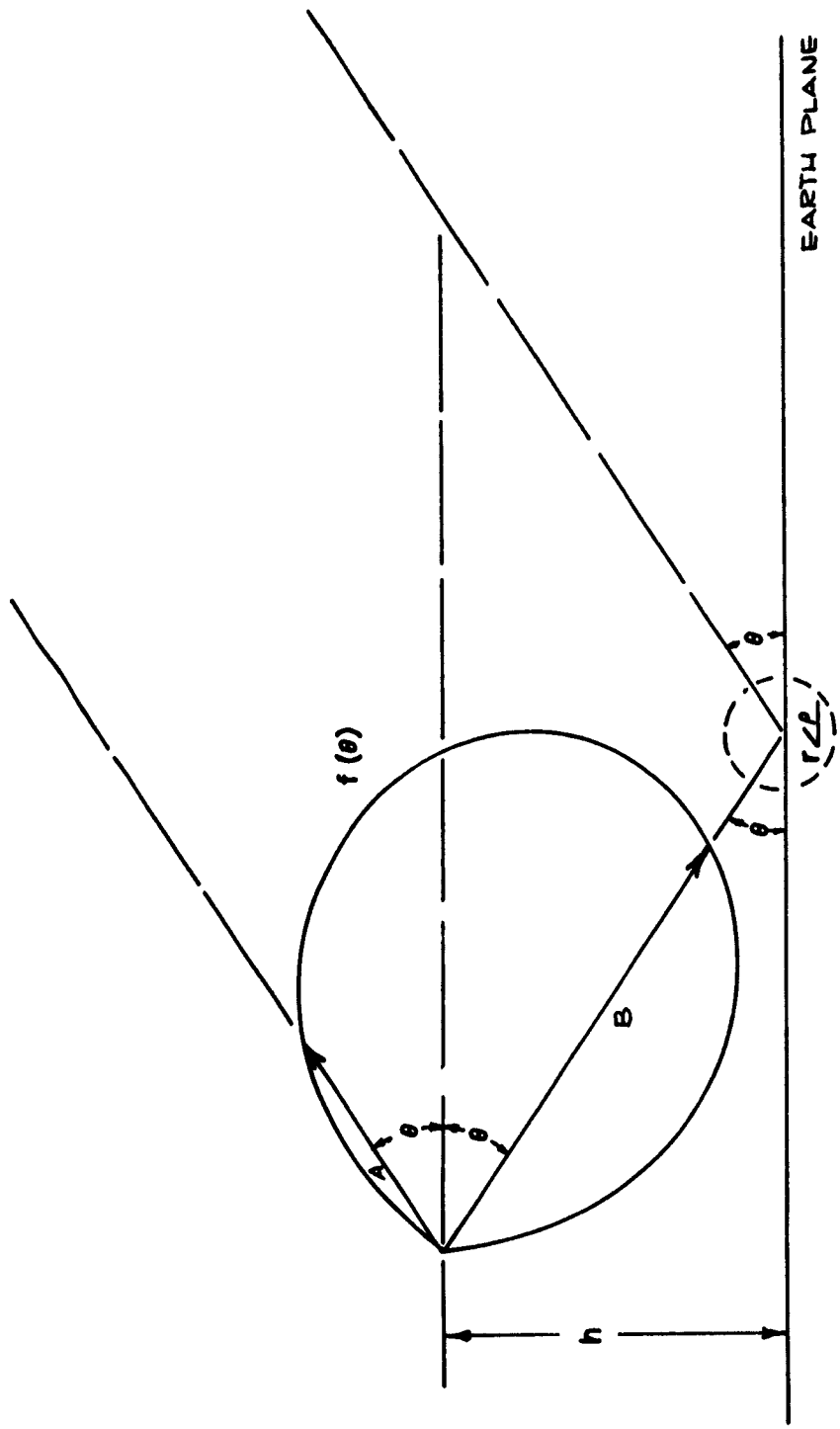

Figure 11. Geometry for calculating effect of imperfect earth on radiation patterns.

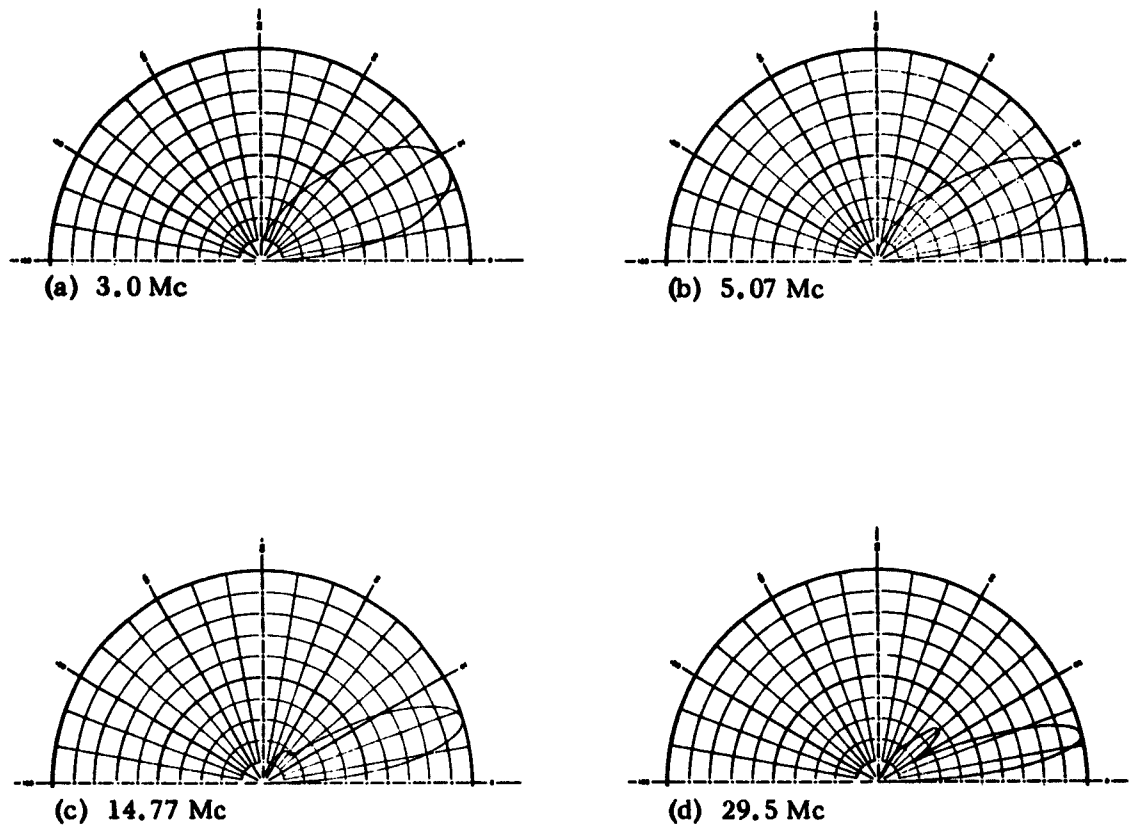

(a) 3.0 Mc

(b) 5.07 Mc

(c) 14.77 Mc

(d) 29.5 Mc

Figure 12. Calculated Elevation Plane Radiation Patterns in Relative Field Strength, 748-3/30-15N Antenna. Imperfect Earth, σ =4 millivolts/meter, ϵ = 10, Assumed.

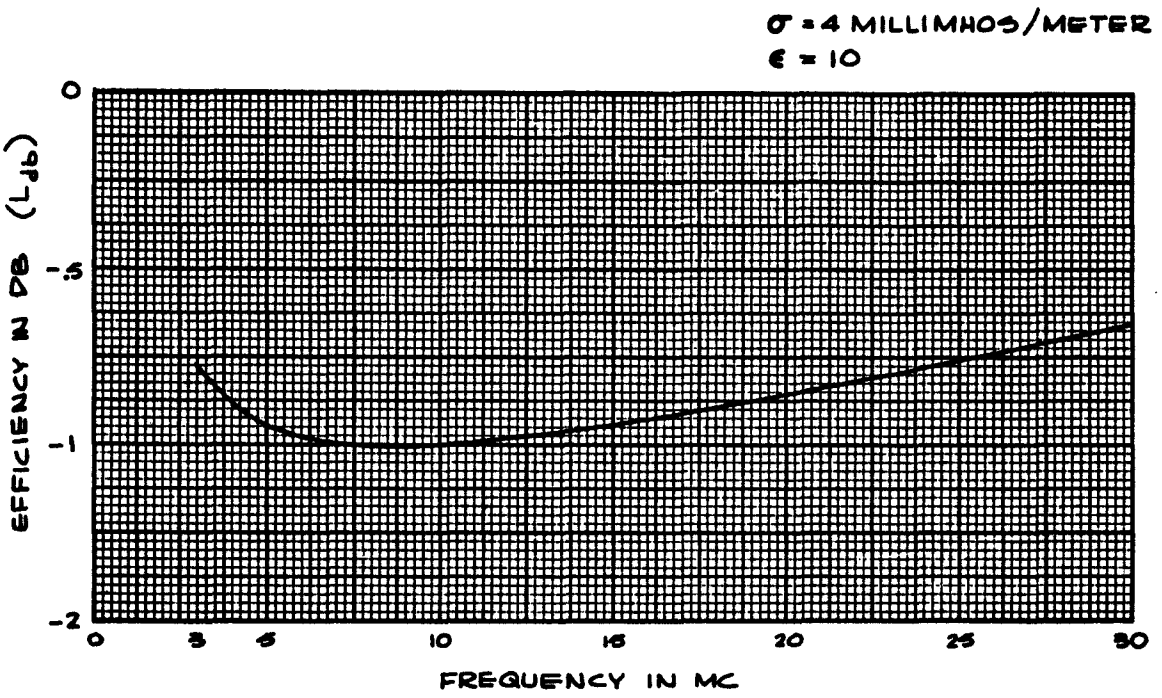

Figure 13. Efficiency due to imperfect earth, 748-3/30-15N Antenna at Barnegat, N. J., compared with performance over perfect earth.

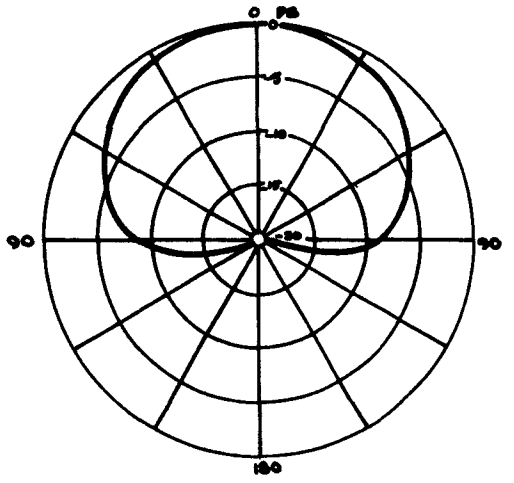

AZIMUTH PLANE RADIATION PATTERN

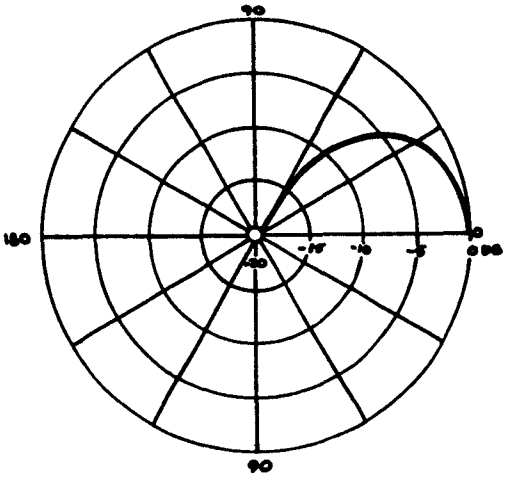

ELEVATION PLANE RADIATION PATTERN OVER PERFECTLY CONDUCTING GROUND

Figure 14. Typical Radiation Patterns, 726-2.5/30-T Antenna. Decibel Plot. Perfect Ground Assumed.

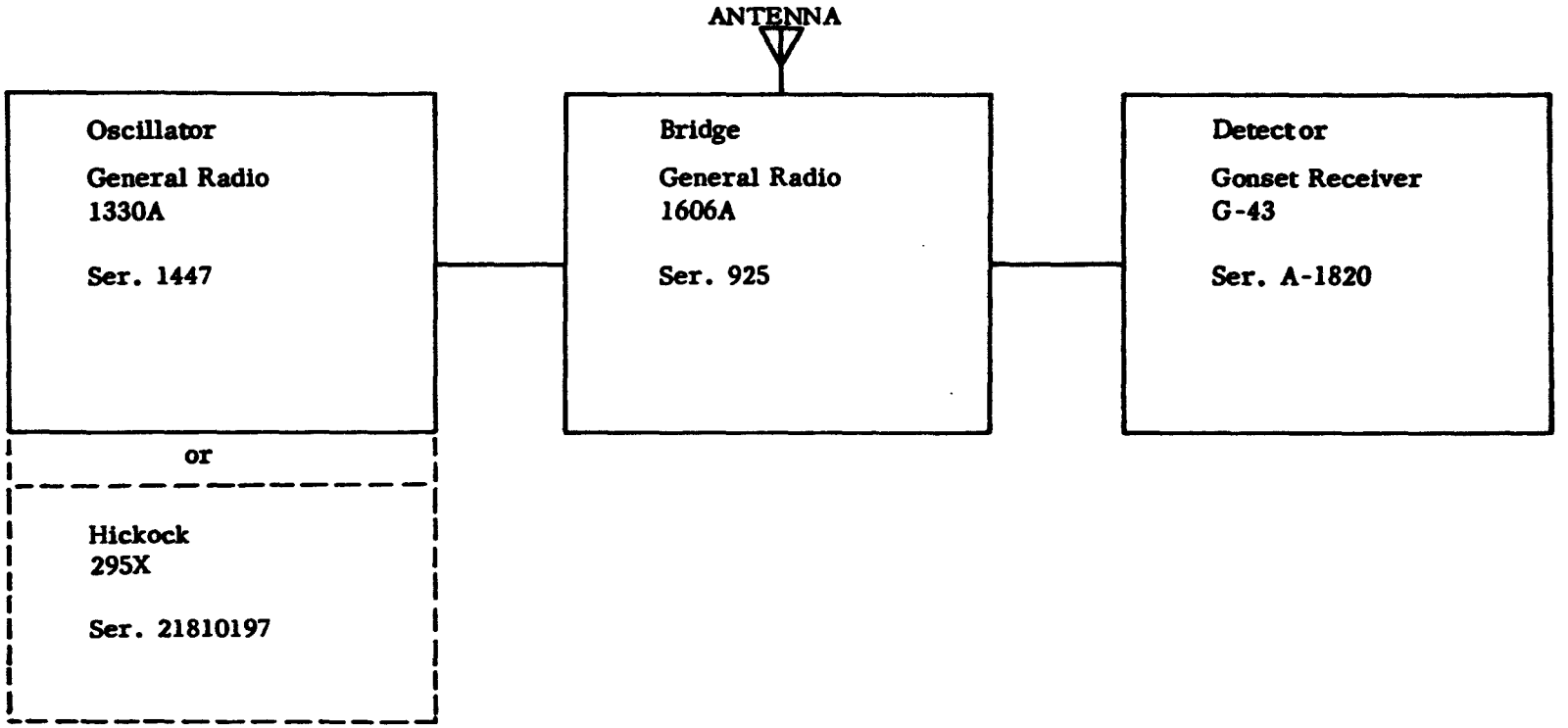

Figure 15. Block Diagram, Test Equipment Used in Impedance Measurements.

FREQUENCY Mc	IMPEDANCE AT ANTENNA, OHMS	IMPEDANCE AT RECEIVER, OHMS
3	39.3 + j 1.33	46 + j 5.0
4	46.3 + j 10.0	
5	55.5 + j 18	38.5 - j 4.6
6	62.5 + j 11.8	
7	71 + j 3.58	
8	63.8 - j 7.5	
9	66.4 - j 6.45	
10	64.2 - j 8.65	53.6 - j 9.5
11	67.5 - j 7.54	
12	67.3 - j 13.9	
13	67.0 - j 13.25	
14	55 - j 27.8	
15	51.6 - j 21.5	61.3 - j 8.15
16	54.8 - j 27.9	
16.5	41.4 - j 32	
17	34.6 - j 22.3	
18	40.0 - j 20.1	
19	45.8 - j 18.85	
19.5	35.9 - j 21	
20	31.8 - j 9.85	47.5 - j 13.25
21	44.5 - j 19.85	
21.5	33.4 - j 19.8	
22	29.8 - j 12.1	
23	34.2 - j 4.09	
24	37.4 - j 1.5	
25	41.1 + j 0.08	48.1 - j 1.8
26	48.3 - j 6.23	
27	41.5 - j 13.4	
28	33.2 - j 8.28	
29	35.3 - j 1.68	
30	41.5 + j 0.8	51.2 - j 1.8

Figure 16. Measured Impedance, 748-3/30-15N Antenna at Barnegat, New Jersey.

FREQUENCY Mc	IMPEDANCE AT ANTENNA, OHMS	IMPEDANCE AT RECEIVER, OHMS
2.5	63.5 + j 35.2	70 + j 28.8
3	73.5 - j 24.7	53 - j 26.3
4	73 - j 6.75	
5	36 + j 4	54 + j 13
6	54 - j 8	
7	47.1 - j 21.4	
8	65.3 + j 1.5	
9	47.4 - j 4.67	
10	57.6 - j 20	36.4 + j 16
11	44.5 - j 2.5	
12	57 - j 18	
13	37.8 - j 6.1	
14	58.4 + j 3.6	
15	56.1 - j 15.3	
16	48.5 - j 7.1	49.6 - j 8.95
17	60.7 - j 16.9	
18	43.8 - j 27.4	
19	29.3 - j 15.7	
20	31.6 + j 3	60 - j 9.6
21	47.7 + j 6.67	
22	53.1 - j 2.5	
23	48.1 - j 5	
24	53.8 + j 2.58	
25	70.2 - j 6.44	51.8 - j 4.64
26	58 - j 31.5	
27	38.7 - j 28.1	
28	25.3 - j 18.6	
29	21.7 - j 4.5	
30	24.4 + j 5.7	79.5 - j 14.8

Figure 17. Measured Impedance, 726-2.5/30-T Antenna at San Juan, Puerto Rico.

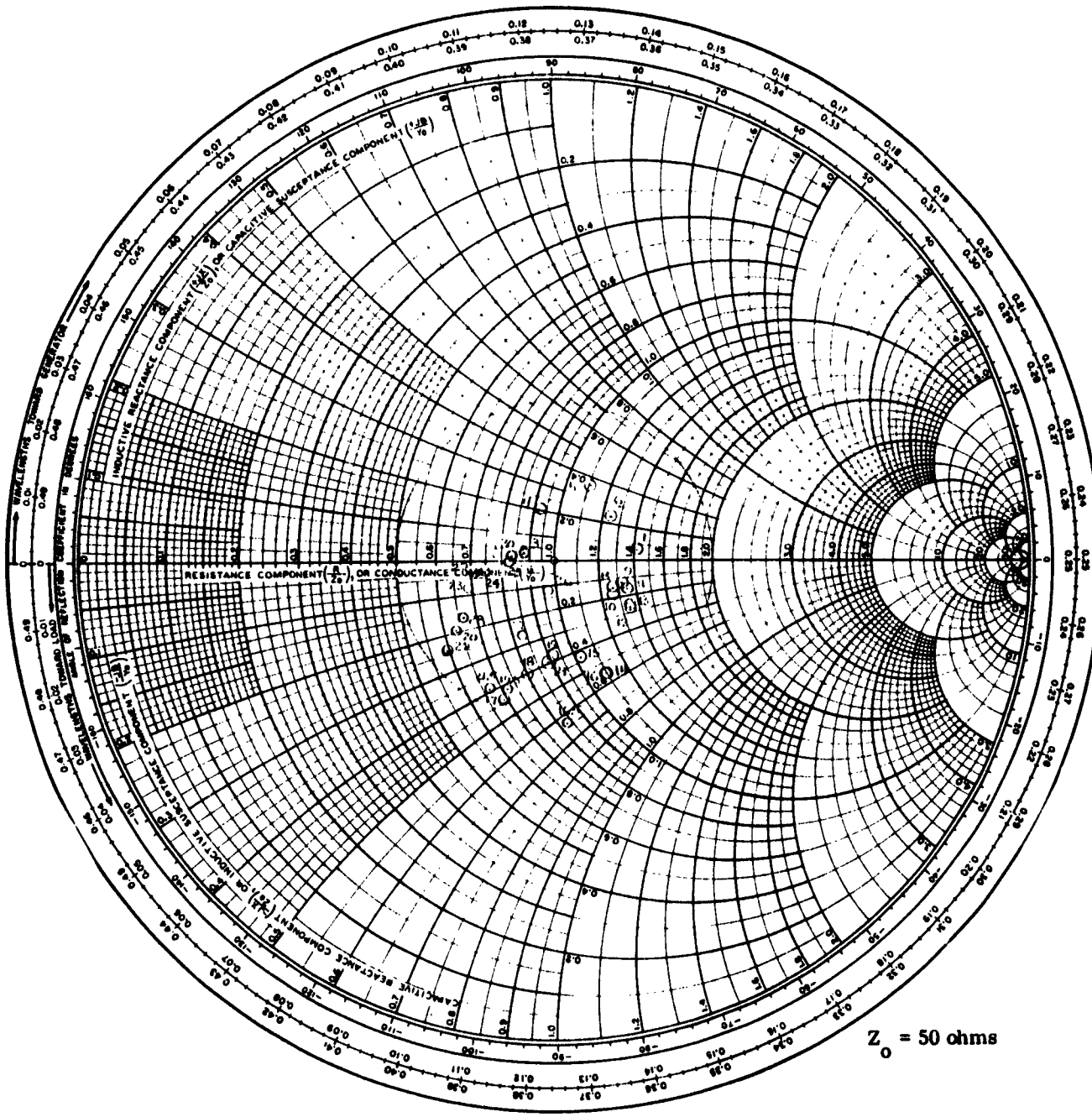

(a) Impedance at Antenna Terminals

Figure 18. Measured Impedance, 748-3/30-15N Antenna at Barnegat, New Jersey.

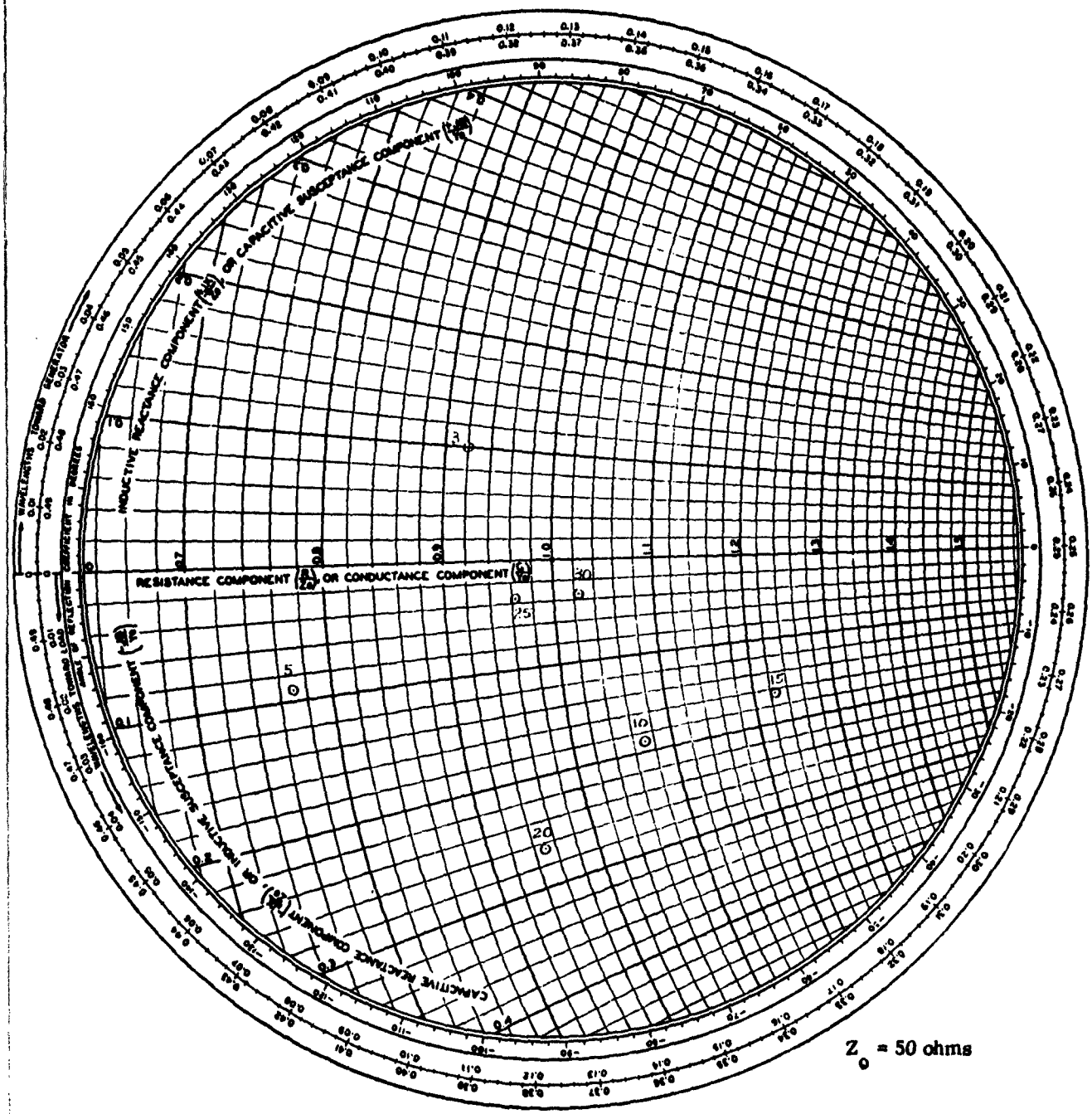

(b) Impedance at Receiver

Figure 18-A. Measured Impedance, 748-3/30-15N Antenna, at Barnegat, New Jersey

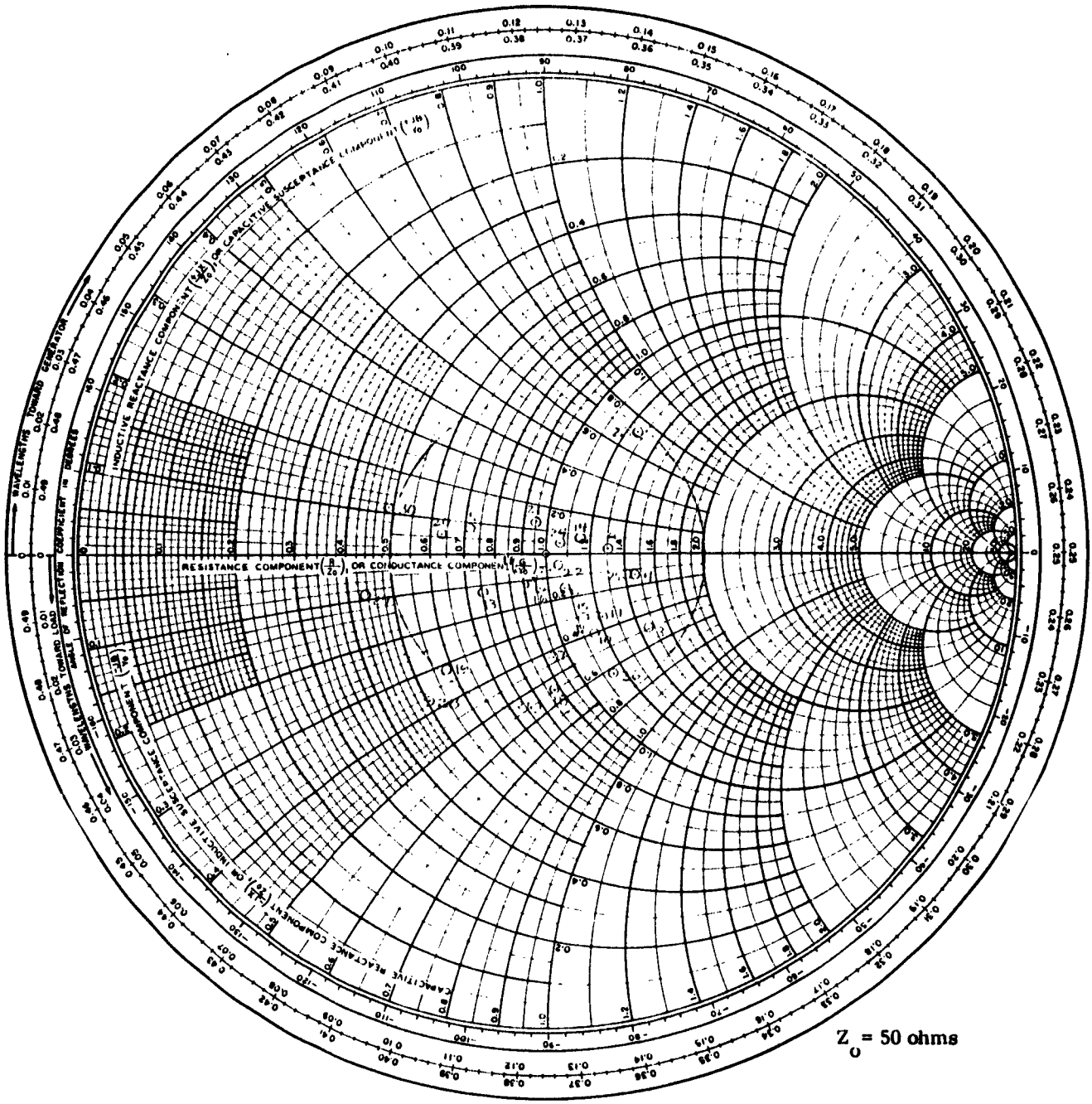

(a) Impedance at Antenna Terminals

Figure 19. Measured Impedance, 726-2.5/30-T Antenna at San Juan, Puerto Rico.

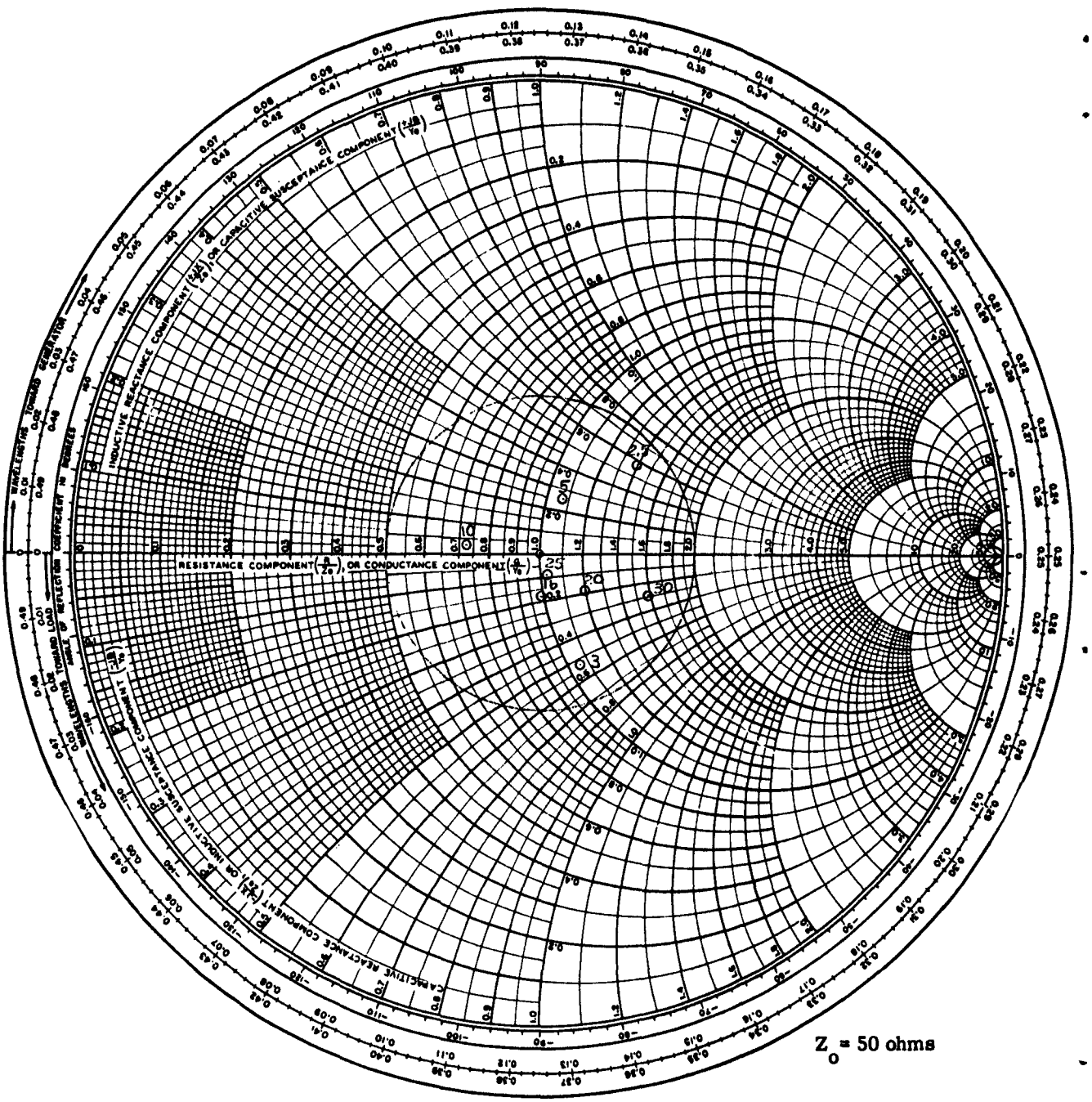

(b) Impedance at Transmitter

Figure 19-A. Measured Impedance, 726-2.5/30-T Antenna at San Juan, Puerto Rico.

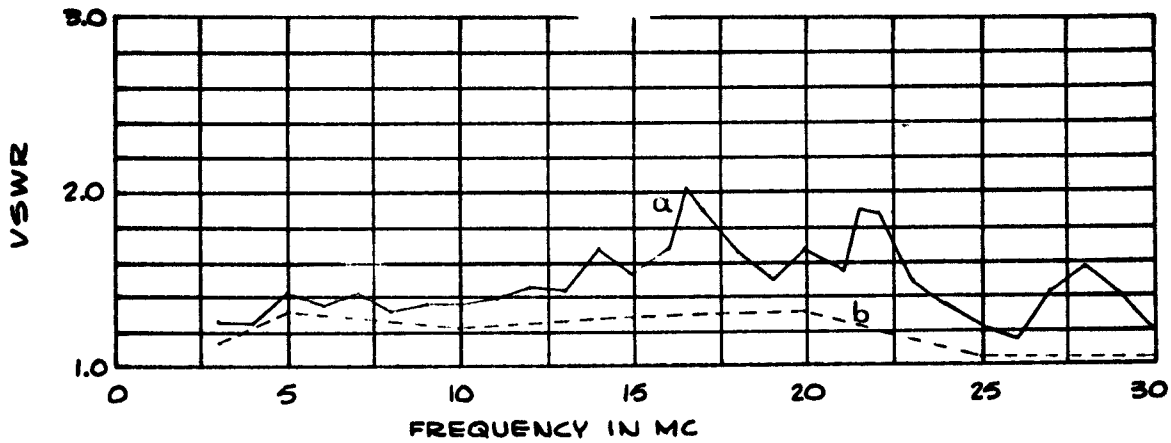

VOLTAGE STANDING WAVE RATIO, 748-3/30-15N
ANTENNA AT BARNEGAT, N.J.
(a) AT ANTENNA
(b) AT RECEIVER

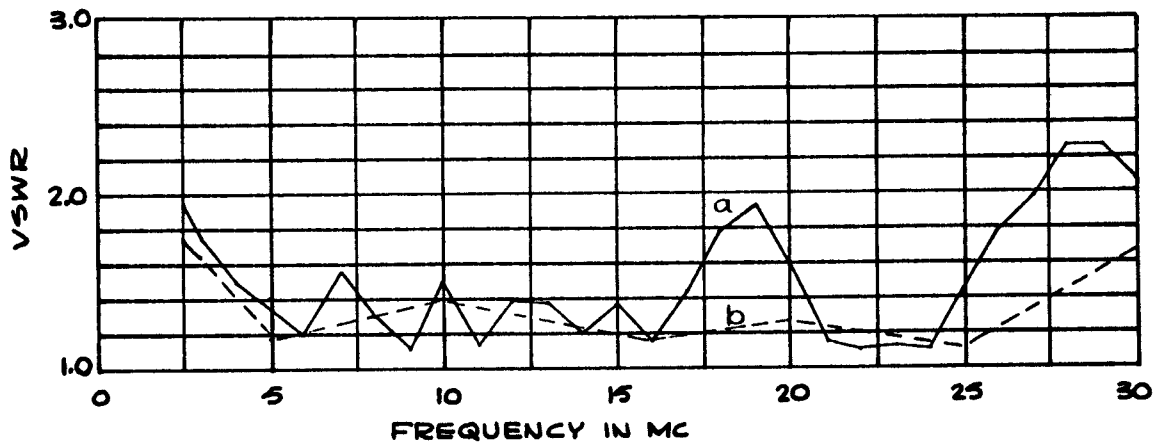

VOLTAGE STANDING WAVE RATIO, 726-2.5/30RT
ANTENNA AT SAN JUAN, P.R.
(a) AT ANTENNA
(b) AT TRANSMITTER

Figure 20. Voltage Standing Wave Ratios

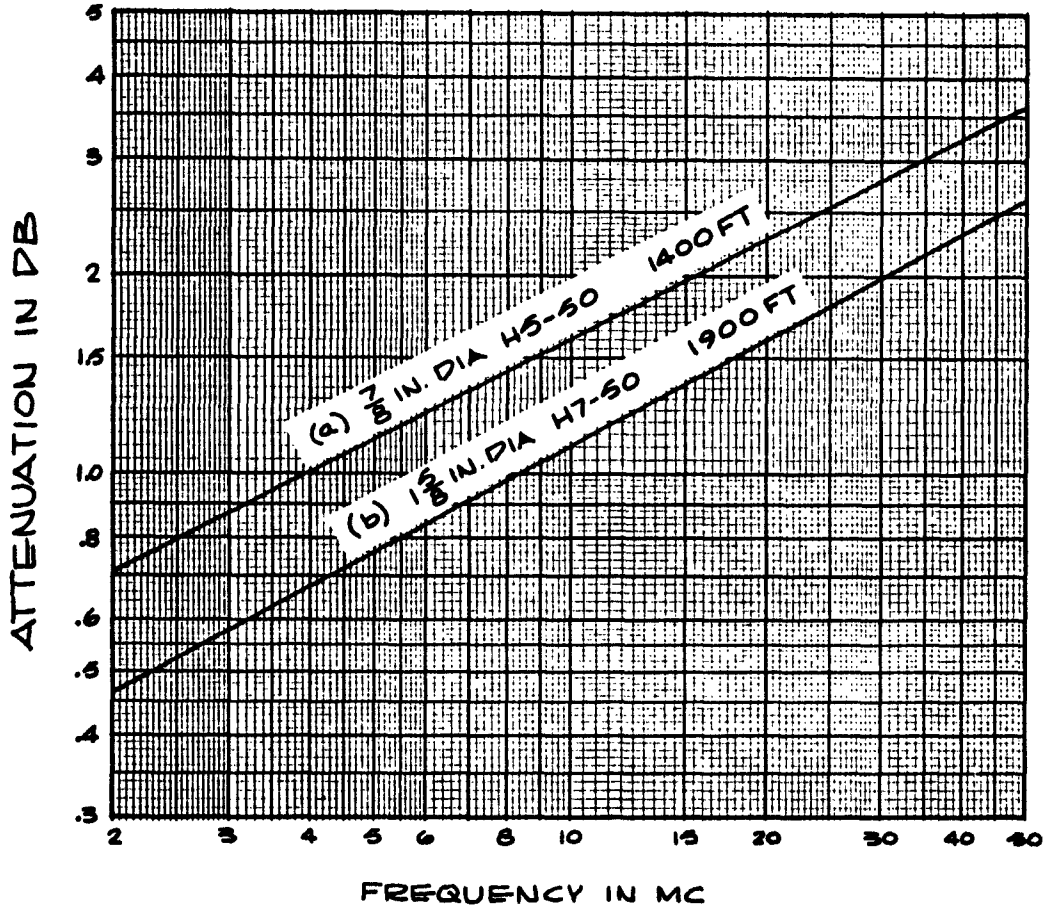

Figure 21. Transmission Line Attenuations.
(a) Barnegat Antenna, (b) San Juan Antenna

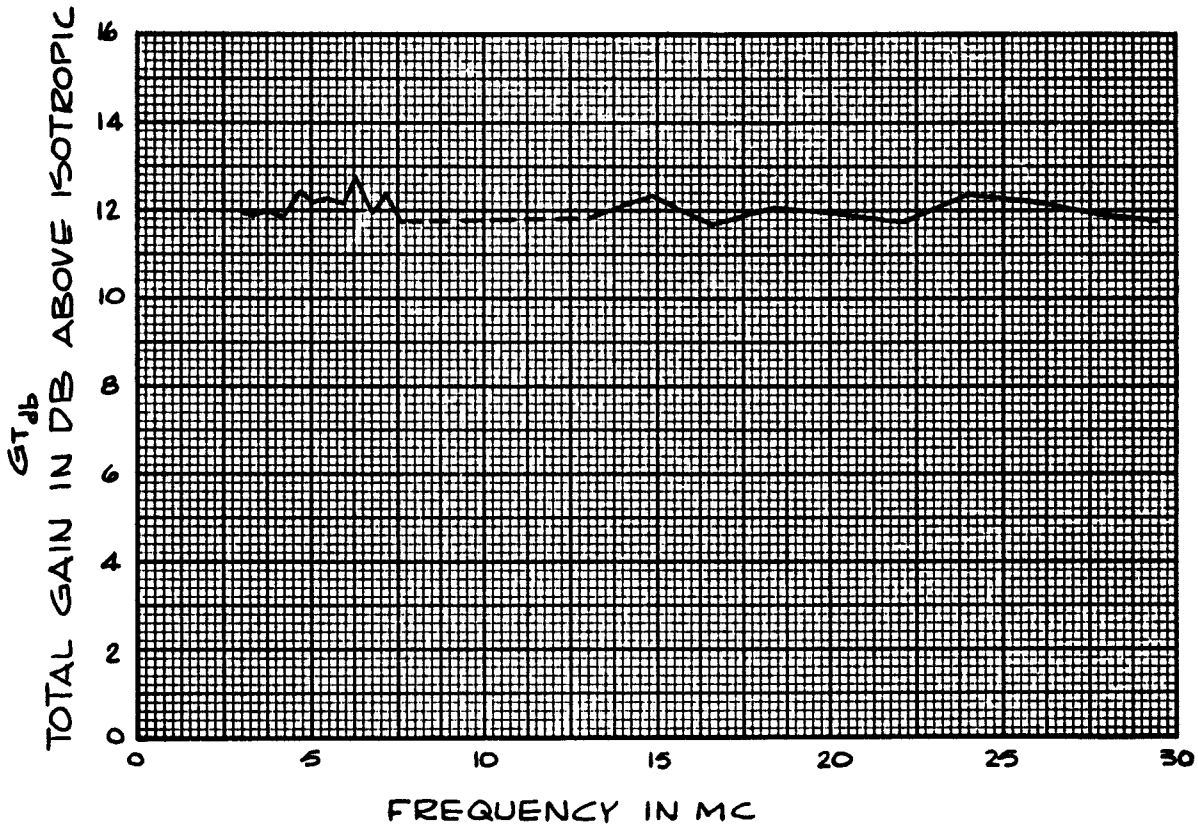

Figure 22. Calculated Total Installed Gain, 748-3/30-15N Antenna at Barnegat, New Jersey.

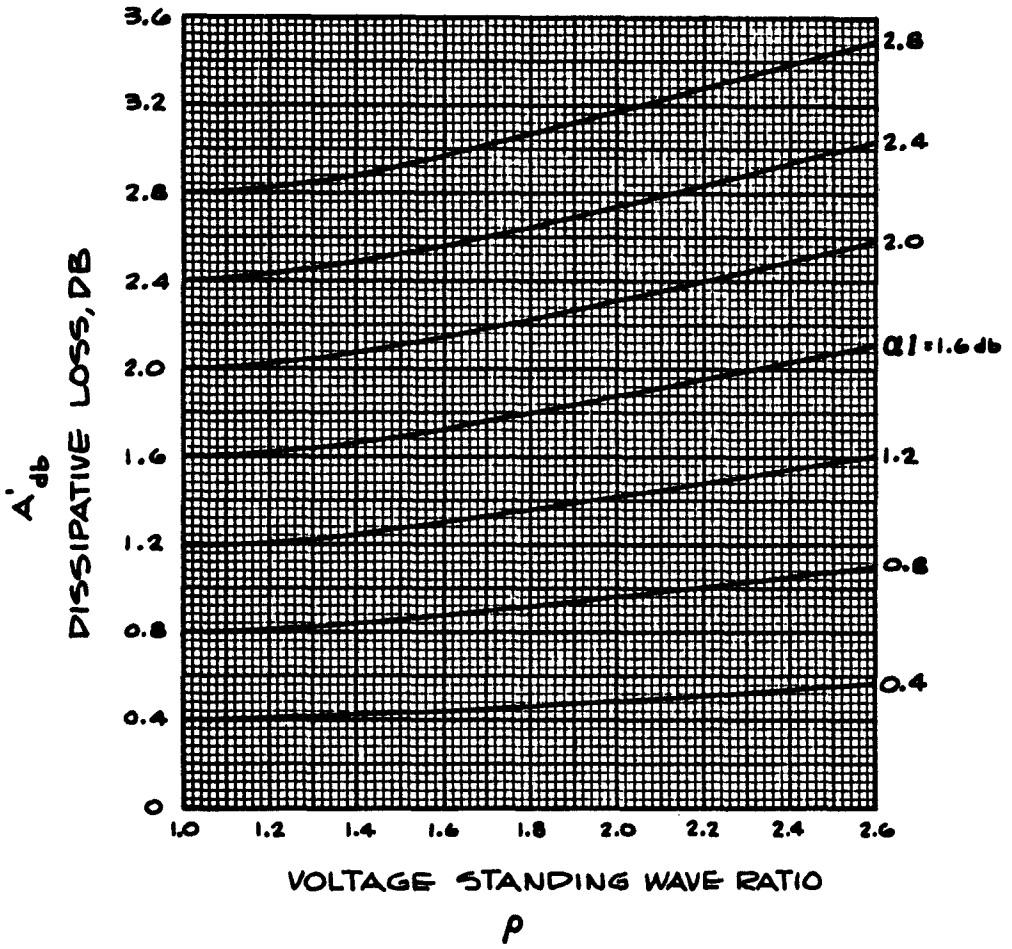

Figure 23. Transmission Line Dissipative Loss As A Function Of Voltage Standing Wave Ratio and Attenuation.

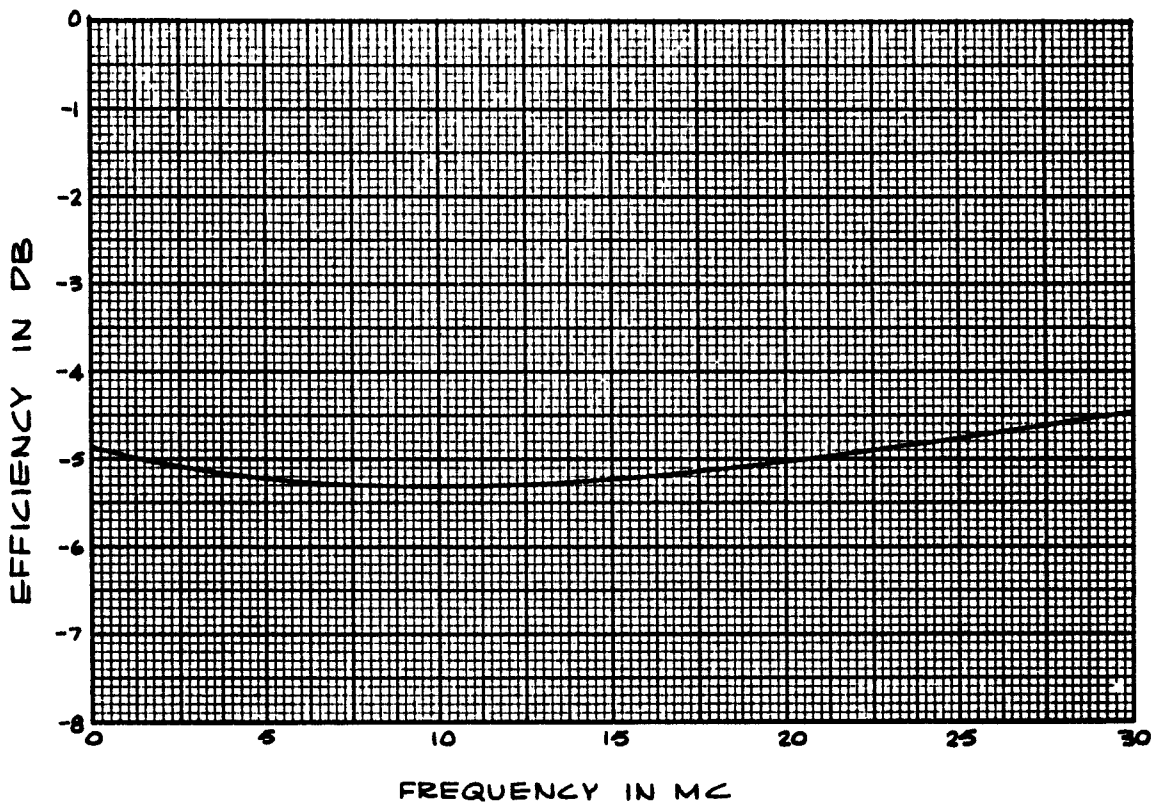

Figure 24. Ground Screen Efficiency, 726-2.5/30-T Antenna, at elevation angle of 8°. Earth constants assumed: σ = 12 millimhos per meter, ϵ = 15.

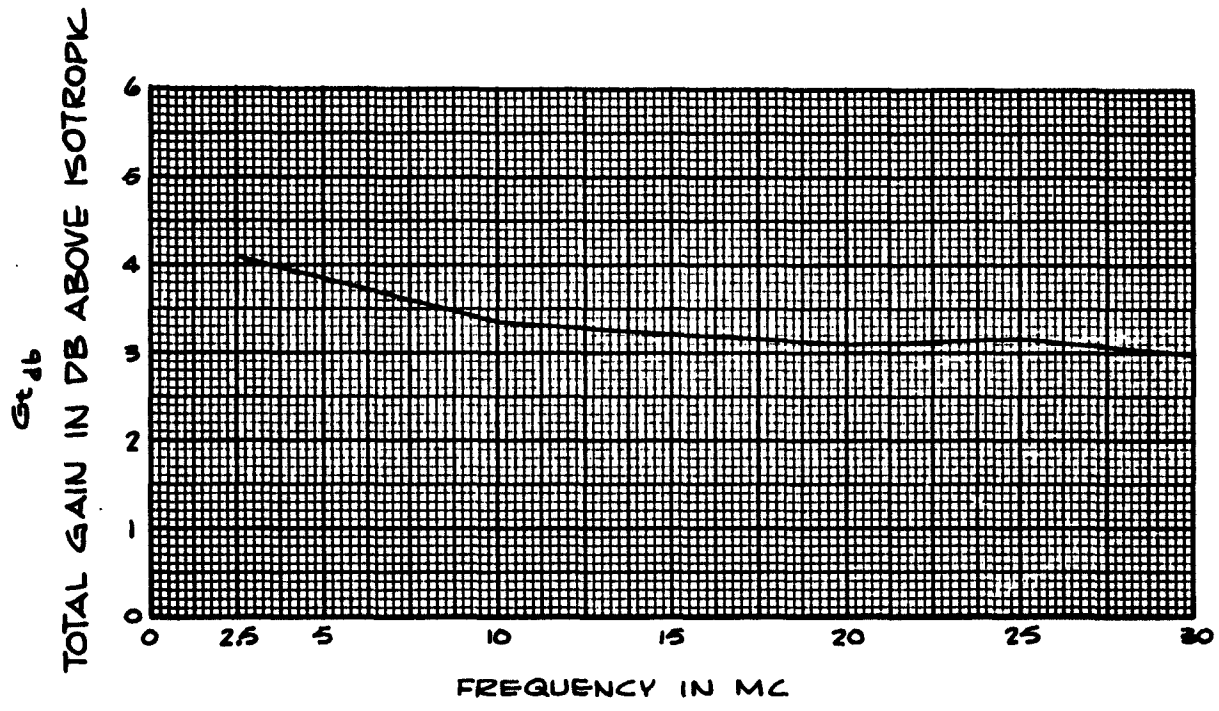

Figure 25. Calculated Total Installed Gain, 726-2.5/30-T Antenna at San Juan, P.R.